A large deformation analysis of plates or membranes for the determination of Young's modulus and Poisson's ratio

Thesis by
Fabienne Breton

In Partial Fulfillment of the Requirements
for the Degree of
Aeronautical Engineer

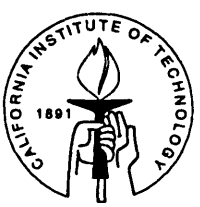

California Institute of Technology
Pasadena, California

1995
(Submitted March 31, 1995)

Acknowledgments

My parents always say that the best years of one's life are university years. People here, at Caltech, have made this statement come true. I would like to thank everybody here, students, faculty and the staff of Galcit for making my stay here most enjoyable. Some individuals, though, taught me more than I could ever expect from a class. I would like to thank in particular Roberto Zenit for supporting and helping me adapt to this new country in my first and difficult year, Mark Walter for being so available to anyone who had an often simple computer question, John Wright and Nicolas Pujet for their friendship and valuable help and finally, my roommate, Ingrid Mounier, for helping me feel that my home was here. I would also like to thank some people who made me a stronger person by demonstrating before my eyes how one can be ill intentioned without a motive. Those three past years have been a "learning experience" in many more fields than my advisor, Professor W. G. Knauss, may think.

All this would not have been possible without the support of my family and also of two very special individuals. I am especially thankful to my parents for their never weakening support, my uncles Jacques et Jean-Louis

Breton for pushing me always further in my studies, Dennis Stanfil for making this dream come true, and finally Jérôme Dessagnat, for convincing me that going away to study was the right choice.

My overall experience at Caltech will leave me with the best memories.

I am deeply grateful to my advisor, Professor W. G. Knauss, for helping instill in me the fundamental concepts of elasticity, during those two years under is guidance as a graduate student and as a teacher assistant.

Finally, the financial support of ONR for the completion of this project is gratefully acknowledged.

Abstract

An analytical method for determining Young's modulus and the Poisson's ratio of thin films is considered; the method is based on the load-deflection behavior of a rectangular membrane of finite aspect ratio $n = b/a$ subjected to uniform pressure (c.f. figure 0.1). Following numerical analysis, previously published model results are shown to be inaccurate, especially for aspect ratios greater than 1.5.

An improved model description decomposes the displacement field into two parts: following the Timoshenko formulation, the deflection is assumed to be sinusoidal near the edges, but for aspect ratios larger than unity the central portion parallel to the longer sides is assumed to bear two-dimensional character (the displacement field is independent of the coordinate parallel to the longer side).

Using energy methods and including the effects of the residual stress, the load-deflection relationship for a rectangular membrane of arbitrary aspect ratio $n = b/a$, under uniform pressure, is obtained.

Experiments are simulated by using numerical analysis. By comparing the numerical data of load-versus-deflection behavior to that for the energy

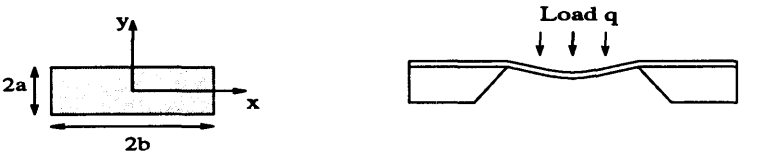

Figure 0.1: Cross-section of sample

based approximation, Young's modulus can be determined to within 2% of the value specified for the numerical analysis, provided that Poisson's ratio, ν, is known. If the latter is not the case, the error increases to 14%, if the full range of Poisson's ratio ($0 \leq \nu \leq 0.5$) is admitted. Narrowing of the uncertainty through bounding Poisson's ratio is demonstrated. This result constitutes a significant improvement over the previous models which were shown to elicit errors on the order of 45%.

A method to evaluate Poisson's ratio is also proposed. Making use of the load-deflection relationship for a rectangular plate of any aspect ratio, Poisson's ratio may be evaluated through the comparison of the load-deflection behavior of membranes of different aspect ratios. This method was found to be valid for materials with Poisson's ratio in the range $\{0.25, 0.5\}$.

Since it is generally difficult to obtain homogeneous films, this study was extended to considerations for bimaterial plates in terms of an effective thickness that is well defined. A layer of the material under examination is deposited onto a well-characterized substrate so that a sandwich film results. Young's modulus of the material can then be deduced from the load-deflection data of the bimaterial film.

Contents

List of Figures

Introduction

Thin films are widely used in the process of producing micro-electronic devices and in micromechanics. It is commonly assumed that the thin film material has mechanical properties identical to those of the bulk material. However, because the ratio of surface to volume of thin film is very high, the question arises of whether this assumption is valid. This question is also important in interface mechanics, when property gradients must exist normal to the interface forming the "contact" between the two materials. This transition region is often considered to be on the order of hundreds or a thousand Ångstrom. In order to investigate the mechanical properties of such a region, it would seem useful to examine the properties of films that are of a thickness with similar or smaller dimensions.

The determination of the physical properties of thin films is typically pursued along two avenues: one way is to use self-supported structures, exemplified by microbridges or membranes. These films are fabricated using photolithography and chemical etching. The film is deposited onto a substrate, after which a part of the substrate is made sensitive to chemical etching by photolithography, leaving a single-layer membrane. The alternative

to this approach is to study films on a supporting microsized structure made of some other material for example, silicon. Both methods have advantages and drawbacks: Using single-layer membranes, the mechanical properties of the thin film itself are measured directly. However, many film materials are not easily produced by etching away their substrate. In that case, measurements on a composite membrane (a film sandwiched with the substrate) may be performed, but results are prone to accuracy limitations because the substrate also influences the overall mechanical behavior of the composite membrane.

Several useful methods have been identified for evaluating the mechanical properties of thin films such as nanoindentation, measurements of the natural frequency of a specimen, measurements of the deflection of buckled membranes, and measurements of the deflection of membranes subjected to uniform pressure. The work presented herein addresses the latter case.

It is the purpose of this study to investigate very compact approximate solutions for the mechanical behavior of thin films. The work was conducted using energy methods, and load-deflection relationships were obtained for different geometries.

The cases of rectangular and circular membranes undergoing large deformation under uniform pressure are studied. In chapter one, the governing equations (Timoshenko) are explored and approximate solutions are found for different geometries. Their limitations in determining Young's modulus and Poisson's ratio are then investigated through comparison with numerical simulations in chapter two. It will also become apparent that Poisson's ratio significantly influences the mechanical behavior of a membrane speci-

men. Motivated by this observation, chapter three explores how geometrical arguments are used to determine Poisson's ratio. Finally chapter four adapts the foregoing analysis to bimaterial membranes, through the use of an appropriately defined "equivalent thickness". It will be shown that for a membrane the "equivalent thickness" should be determined by a tension-equivalent while a bending-equivalent is appropriate for small deformation resulting from plate bending. This latter observation reinforces the assumption that the mechanical behavior of membranes is driven by in-plane stretching rather than by resistance to bending.

Chapter 1

Approximate solutions for the large deformation of membranes

In this chapter, the approximate solutions for large deformations of membranes under uniform pressure will be investigated. In Section 1.1, some hypothesis on the membrane itself and on the membrane behavior will be formulated. Section 1.2 presents the general method to obtain a load-deflection relationship for membranes of any geometry. This method will then be applied to a square membrane in Section 1.3, an infinite strip in Section 1.4, a rectangular membrane of finite aspect ratio in Section 1.5 and finally to a circular membrane in Section 1.6.

1.1 Hypotheses

In the sequel, the assumptions and definitions necessary to formulate the membrane theory are presented.

1.1.1 Thickness change

To observe the load-deflection behavior of a thin film the thickness of which is typically on the order of a few nanometers ($10^{-9}\,m$), the specimen must sustain deflections many times larger than its thickness. To remain in the range of linearly elastic material behavior, the deflection should be such that the engineering strain in the film is typically less than 0.2% (c.f. Section 2.4). By assuming a perfectly cylindrically deformed shape, one can easily approximate the value of the engineering strain as a function of the deflection, using simple trigonometric arguments (c.f. Figure 1.1),

$$\begin{aligned} \varepsilon &= \frac{R\theta}{a} - 1 \\ &= \left(\frac{w_0^2 + a^2}{2aw_0}\right) \arcsin\left(\frac{2aw_0}{w_0^2 + a^2}\right) - 1, \end{aligned}$$

where a is half of the characteristic length and w_0 is the maximal deflection. This can be further approximated by

$$\varepsilon \sim \frac{2}{3}\left(\frac{w_0}{a}\right)^2. \tag{1.1}$$

Thus, in order to work in the linearly elastic range, the central deflection should not exceed $0.05 \times a$. As long as that condition is obeyed, one

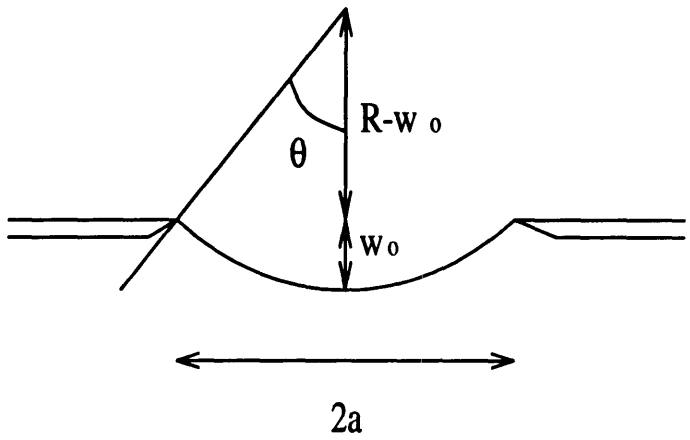

Figure 1.1: Geometric parameters for engineering strain calculation

may assume that there is also no significant change in the thickness of the membrane.

Note that even though the material is considered linearly elastic (less than 0.2% strain), the deformation is considered large because the deflection is much larger than the thickness of the membrane.

1.1.2 Film manufacturing

There exist several techniques to manufacture thin films, such as vapor deposition or chemical etching. However, every method is known to induce some residual stresses in the final membrane. These will have to be accounted for when one writes the (differential) equilibrium equation for an assumed isotropic material. To that end, one writes the net forces as

$$\begin{aligned} N_x^{total} &= N_x + h(\sigma_x)_0 \\ N_y^{total} &= N_y + h(\sigma_y)_0 \end{aligned} \tag{1.2}$$

$$N_{xy}^{total} = N_{xy} + h(\sigma_{xy})_0$$

where N_α is the force per unit length in the α-th direction, $(\sigma_\alpha)_0$ is the residual stress in the α-th direction and h is the thickness of the film. It will be assumed that the residual stresses $(\sigma_\alpha)_0$ are spatially constant. Moreover, the shear strain $(\sigma_{xy})_0$ is taken to be zero.

1.1.3 Membrane behavior

Thin films may be viewed as plates with a thickness tending to zero. As a result, their flexural rigidity tends to zero as well. Therefore, the load-deflection behavior is governed by the stretching of the middle plane rather than by the resistance to bending. Consequently, the contribution of the resistance to bending will be neglected.

1.1.4 Applied pressure

The membranes considered are under uniform pressure. The load is, therefore, always perpendicular to the membrane. The method developed in this section will assume that the load is along the z-axis.

1.2 General method

From intuition, one can assume a functional form for the components of the displacement field $u(x, y, z)$, $v(x, y, z)$ and $w(x, y, z)$ that satisfies the boundary conditions.

The resulting large deformation strains are computed using the simplification introduced by Timoshenko [1].

$$\begin{aligned} \epsilon_x &= \frac{\partial u}{\partial x} + \frac{1}{2}(\frac{\partial w}{\partial x})^2 \\ \epsilon_y &= \frac{\partial v}{\partial y} + \frac{1}{2}(\frac{\partial w}{\partial y})^2 \\ \gamma_{xy} &= \frac{\partial u}{\partial y} + \frac{\partial v}{\partial x} + \frac{\partial w}{\partial x}\frac{\partial w}{\partial y}. \end{aligned} \tag{1.3}$$

Note that in the following study, the in-plane strain should not exceed 0.2% and the non-linear terms are probably negligible.

If the plate is linearly elastic, the following strain-force relations govern

$$\begin{aligned} \epsilon_x &= \frac{1}{h\,E}(N_x - \nu N_y) \\ \epsilon_y &= \frac{1}{h\,E}(N_y - \nu N_x) \\ \gamma_{xy} &= \frac{1}{2\,h}\frac{N_{xy}}{E(1+\nu)} \end{aligned} \tag{1.4}$$

From the above, the strain energy, V, is evaluated as

$$V = \int_A \{\int_0^{\epsilon_x} N_x^t d\epsilon_x + \int_0^{\epsilon_y} N_y^t d\epsilon_y + \int_0^{\gamma_{xy}} N_{xy}^t d\gamma_{xy}\} dx\, dy$$

which can be rewritten as

$$V = V_e + V_r$$

where V_e is the strain energy due to the loading and V_r is the strain energy

due to the residual stresses in the membrane. V_e and V_r are then given by

$$\begin{aligned} V_e &= \frac{1}{2}\int_A (N_x\epsilon_x + N_y\epsilon_y + N_{xy}\gamma_{xy})dx\,dy, \\ V_r &= \frac{h}{2}\int_A (\sigma_x)_0\epsilon_x + (\sigma_y)_0\epsilon_y\,dx\,dy. \end{aligned}$$

Making use of Equation 1.4, one obtains the elastic strain energy as a function of the strains only, namely

$$V_e = \frac{Eh}{2(1-\nu^2)}\int_A (\epsilon_x^2 + \epsilon_y^2 + 2\nu\epsilon_x\epsilon_y + \frac{1}{2}(1-\nu)\gamma_{xy}^2)dx\,dy. \qquad (1.5)$$

The potential energy, Π, is then

$$\Pi = V - \int_A q\,w(x,y)\,dx\,dy. \qquad (1.6)$$

The unknown constants in the displacement field and the desired load-deflection relationship are derived using the potential energy minimization theorem.

The success of this method depends on the form of the assumed displacement field. A value of the potential energy Π may be calculated from any admissible function and then minimized with respect to the unknown constants. However, Π is an absolute minimum only if the displacement field is exact. Thus, pick a simple but very reasonable deformation pattern that closely approximates the exact solution. One may then check on closeness by comparing with numerical data.

1.3 Application to a square plate

This method is first applied to determine the load-deflection behavior of a square plate [2]. Assume the following displacement field,

$$\begin{aligned} u &= c\sin(\frac{\pi x}{a})\cos(\frac{\pi y}{2a}), \\ v &= c\sin(\frac{\pi y}{a})\cos(\frac{\pi x}{2a}), \\ w &= w_0\cos(\frac{\pi x}{2a})\cos(\frac{\pi y}{2a}), \end{aligned} \tag{1.7}$$

and compute the total strain energy,

$$V = \frac{\pi^2}{8}\sigma_0 h w_0^2 + \frac{E\,h}{2(1-\nu^2)}(rc^2 + s\frac{c}{a}w_0^2\pi^2 + \frac{5\pi^4}{256}\frac{w_0^4}{a^2}) \tag{1.8}$$

where

$$\begin{aligned} r &= \frac{16}{9}(1+\nu) + \frac{\pi^2}{4}(9-\nu), \\ s &= \frac{-5+3\nu}{6}. \end{aligned} \tag{1.9}$$

From Equation 1.6, compute the total potential energy,

$$\Pi = \frac{\pi^2}{8}\sigma_0 h w_0^2 + \frac{E\,h}{2(1-\nu^2)}(rc^2 + s\frac{c}{a}w_0^2\pi^2 + \frac{5\pi^4}{256}\frac{w_0^4}{a^2}) - 16\frac{a^2 q w_0}{\pi^2}.$$

First minimize Π with respect to c and obtain c as a function of w_0. Then, minimize Π with respect to w_0, substitute c by its value and obtain the

following load-deflection relation

$$\frac{\pi^4}{64}\sigma_0\frac{hw_0}{a^2}+\frac{\pi^6}{32}(\frac{5}{64}-\frac{s^2}{r})\frac{E}{(1-\nu^2)}\frac{hw_0^3}{a^4}=q \tag{1.10}$$

1.4 Application to an infinite strip

In the case of an infinite strip, the problem is one-dimensional and the governing equations are greatly simplified. It is possible in that case to find the exact solution. The displacement field is found to be a superposition of a hyperbolic cosine function and a parabolic function. Their respective amplitude cannot, however, be found in closed form since they are roots of a transcendental equation. The search of an approximate solution is therefore justified by its more compact form.

The displacement field will be approximated by sine and cosine functions as follows

$$\begin{aligned} u &= c\sin(\frac{\pi x}{a}), \\ w &= w_0\cos(\frac{\pi x}{2a}). \end{aligned} \tag{1.11}$$

Computing and minimizing the total potential energy Π (per unit length) yields the desired load-deflection relationship.

$$\begin{aligned} V &= \frac{E\pi^2 h}{8a^3(1-\nu^2)}\left(4a^2c^2-\frac{1}{2}ac\pi {w_0}^2+\frac{3}{64}\pi^2 {w_0}^4\right)+\pi^2\sigma_0\frac{h{w_0}^2}{16a} \\ \Pi &= V-\frac{4}{\pi}aqw_0 \end{aligned} \tag{1.12}$$

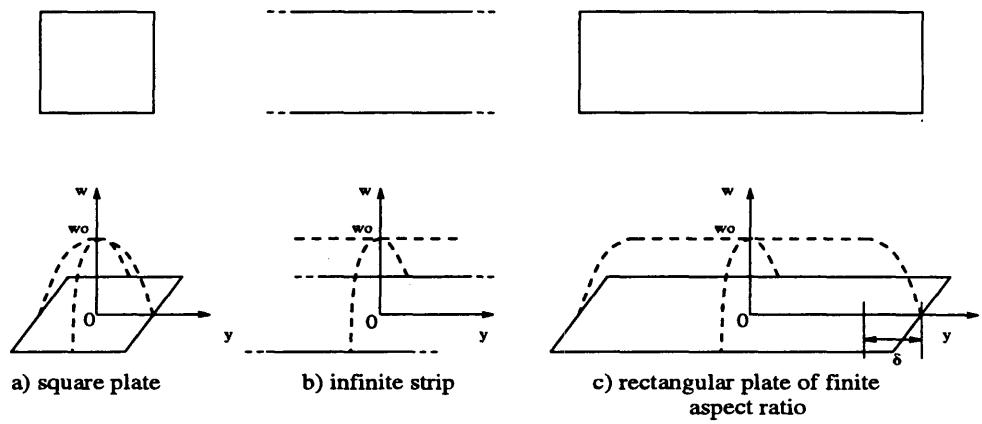

Figure 1.2: Shape of the deflection for different aspect ratios

Therefore, minimization of Π with respect to c and w_0 yields

$$\frac{\pi^3}{32}\frac{h}{a^2}\sigma_0 w_0 + \frac{\pi^5}{256}\frac{E}{(1-\nu^2)}\frac{h w_0^3}{a^4} = q \tag{1.13}$$

1.5 Rectangular plate of finite aspect ratio

From intuition, one can think that a rectangular plate of finite aspect ratio will behave neither like a square plate (sinusoidal displacement field) nor like an infinite strip (constant central deflection), but rather like a combination of both (Figure 1.2). Thus, using the mathematical properties of the potential energy (namely additivity and non-dependence on coordinate system), one can calculate the strain energy of a rectangular membrane of aspect ratio b/a described by a displacement field that takes those two aspects under consideration. By symmetry, the problem can be reduced to the study of one half of the plate. In Section 1.5.1, the distance δ at which the "short" edges cease to influence the membrane behavior will be assumed to be equal to the

half length a. In Section 1.5.2, it will be assumed that this distance is some fraction k of a.

1.5.1 Assume that $\delta = a$

First assume that the distance at which the edges cease to influence the behavior of the membrane is $\delta = a$. The displacement field is then decomposed in two parts:

- For $y \in [0, (b-a)]$:

  Assume that the membrane behaves like an infinite strip. Thus, the displacement field does not depend on y, but only on x. Moreover, assume that the displacement field has no component in the y-direction, namely $v(x) = 0$. Take

$$\begin{cases} u^I(y) = c\sin(\frac{\pi x}{a}) \\ w^I(y) = w_0\cos(\frac{\pi x}{2a}) \end{cases}$$

- For $y \in [(b-a), b]$:

  Assume that this part behaves like a square plate and

$$\begin{cases} u(x,y)^{II} = c\sin(\frac{\pi x}{a})\cos\frac{\pi}{2a}(y-(b-a)) \\ v(x,y)^{II} = c\cos(\frac{\pi x}{2a})\sin\frac{\pi}{a}(y-(b-a)) \\ w(x,y)^{II} = w_0\cos(\frac{\pi x}{2a})\cos\frac{\pi}{2a}(y-(b-a)) \end{cases}$$

The system is, therefore, described by the following

$$u(x,y) = \begin{cases} c\sin(\frac{\pi x}{a}) & y \in [0,(b-a)] \\ c\sin(\frac{\pi x}{a})\cos\frac{\pi}{2a}(y-(b-a)) & y \in [(b-a),b] \end{cases}$$

$$v(x,y) = \begin{cases} 0 & y \in [0,(b-a)] \\ c\cos(\frac{\pi x}{2a})\sin\frac{\pi}{a}(y-(b-a)) & y \in [(b-a),b] \end{cases}$$

$$w(x,y) = \begin{cases} w_0\cos(\frac{\pi x}{2a}) & y \in [0,(b-a)] \\ w_0\cos(\frac{\pi x}{2a})\cos\frac{\pi}{2a}(y-(b-a)) & y \in [(b-a),b] \end{cases}$$

Note that the above displacements are continuous at $x = b-a$ and vanish at the edges.

The strain energy is the sum of the strain energy of a rectangular plate with two free edges of length $(b-a)$ (whose behavior is similar to that of an infinite strip) and one half of the strain energy of a square membrane of side $2a$ (Equation 1.8), namely

$$\begin{aligned} V &= \frac{\pi^2}{16}\sigma_0 h w_0^2 + \frac{E\,h}{4(1-\nu^2)}\left(rc^2 + s\frac{c}{a}w_0^2\pi^2 + \frac{5\pi^4}{256}\frac{w_0^4}{a^2}\right) \\ &+ (b-a)\frac{E\pi^2 h}{8a^3(1-\nu^2)}\left(4a^2c^2 - \frac{1}{2}ac\pi {w_0}^2 + \frac{3}{64}\pi^2 {w_0}^4\right) + \pi^2\sigma_0\frac{h{w_0}^2}{8}\frac{(b-a)}{a} \end{aligned}$$

Substitute the aspect ratio b/a by n and simplify to obtain

$$\begin{aligned} V &= n\frac{\pi^2}{16}\sigma_0 h w_0^2 + \frac{E\,h}{4(1-\nu^2)}\left(rc^2 + s\frac{c}{a}w_0^2\pi^2 + \frac{5\pi^4}{256}\frac{w_0^4}{a^2}\right) \\ &+ (n-1)\frac{E\,h}{(1-\nu^2)}\frac{\pi^2}{8}\left(4c^2 - \frac{1}{2}\frac{c}{a}\pi w_0^2 + \frac{3}{64}\pi^2\frac{w_0^4}{a^2}\right) \end{aligned}$$

where r and s were defined in 1.9. Note that for $n = 1$, one retrieves, as expected, the value of the strain energy of a square membrane of side $2a$.

To obtain the potential energy Π, one needs to compute the work $\mathcal{W}$ done by the load, which is

$$\begin{aligned} \mathcal{W} &= \int_A q\,w(x,y)\,dx\,dy \\ &= \int_{-a}^{a}\int_{0}^{(b-a)} q\,w^I(x,y)\,dx,dy + \int_{-a}^{a}\int_{(b-a)}^{b} q\,w^{II}(x,y)\,dx,dy \\ &= \frac{qa^2}{\pi}\left(\frac{8}{\pi} + 4(n-1)\right)w_0 \end{aligned}$$

Then, minimize Π

$$\Pi = V - \mathcal{W}$$

with respect to c and w_0 to obtain the desired load-deflection relationship

$$n\frac{\pi^3}{8}\sigma_0\frac{hw_0}{a^2} + \frac{E\pi^5}{4(1-\nu^2)}\frac{hw_0^3}{a^4}\left(\frac{6n-1}{64} - \frac{(s-\frac{\pi}{4}(n-1))^2}{r+2\pi^2(n-1)}\right) = q\left(\frac{8}{\pi} + 4(n-1)\right), \tag{1.14}$$

where r and s are given by Equation 1.9. Note that if $n = 1$, Equation 1.14 is similar to Equation 1.10, as expected.

1.5.2 Assume that $\delta = k\,a$

Take $\delta = k\,a$ (where k is expected to be on the order of one), and minimize the potential energy with respect to c, w_0 and k. To achieve this, the membrane has to be decomposed into two parts again: a portion of length $(b - k\,a)$ that will behave like an infinite strip, and a rectangular portion of sides $2a \times 2\,k\,a$, for which the displacement field will be assumed to be sinusoidal. Neglecting the residual stress σ_0 (cf. Section 2.3), the strain energy of one half of the plate is

$$V = \frac{E\,h}{(1-\nu^2)}\left\{c^2 r' + \frac{\pi^2 w_0^2 c}{ak}s' + \frac{\pi^4 w_0^4}{k^3 a^2}l'\right\}$$

with

$$\begin{aligned} r' &= \left(\frac{4}{9}(1+\nu) + \frac{\pi^2}{k}(1+k^2)\left(\frac{9-\nu}{32}\right) + \frac{\pi^2}{2}(n-k)\right) \\ s' &= \left(\left(\frac{-1+3\nu-4k^2}{48}\right) + \frac{1}{k}\left(k^2\left(\frac{3\nu-1}{48}\right) - \frac{1}{12}\right) - \frac{\pi k}{16}(n-k)\right) \\ l' &= \left(\frac{9}{4096}(1+k^4) + \frac{k^2}{2048} + \frac{3}{512}k^3(n-k)\right). \end{aligned}$$

The work done by the load is

$$\mathcal{W} = \frac{q w_0 a^2}{\pi}\left(\frac{8k}{\pi} + 4(n-k)\right).$$

Therefore, the potential energy becomes

$$\Pi = \frac{E\,h}{(1-\nu^2)}\left\{c^2 r' + \frac{\pi^2 w_0^2 c}{ak}s' + \frac{\pi^4 w_0^4}{k^3 a^2}l'\right\} - \frac{q w_0 a^2}{\pi}\left(\frac{8k}{\pi} + 4(n-k)\right).$$

Minimizing Π with respect to c and w_0 in closed form yields

$$\begin{aligned} \frac{\partial \Pi}{\partial c} &= 0 \Longrightarrow c = -\frac{\pi^2 w_0^2}{ak}\frac{s'}{2r'} \\ \frac{\partial \Pi}{\partial w_0} &= 0 \Longrightarrow w_0 = \alpha_k a \sqrt[3]{\frac{aq}{Eh}} \end{aligned}$$

where

$$\alpha_k = \left\{ \frac{4(1-\nu^2)k^2}{\pi^5} \frac{\left(\frac{2k}{\pi} + (n-k)\right)}{\frac{4l}{k} - \frac{s'^2}{r'}} \right\}^{1/3}.$$

To obtain the value of $k^\star$ that minimizes the potential energy, plot the value of Π as a function of k for different aspect ratios (see Figures 1.3, 1.4, 1.5).

As expected, $k^\star$ is close to unity for aspect ratios two, four and ten. Variations of $k^\star$ as a function of the aspect ratio are shown in Figure 1.6.

1.6 Application to a circular plate

Let a circular membrane of radius a and thickness h be subjected to a uniform pressure q. Assuming that the shape of the deflected surface can be represented by the same equation as in the case of small deformations, choose the following displacement field:

$$\begin{aligned} u &= r(a-r)(c_1 + c_2 r), \qquad (1.15) \\ w &= w_0(1 - \frac{r^2}{a^2})^2. \end{aligned}$$

From equations 1.15, one calculates the strain components ϵ_r and ϵ_t in

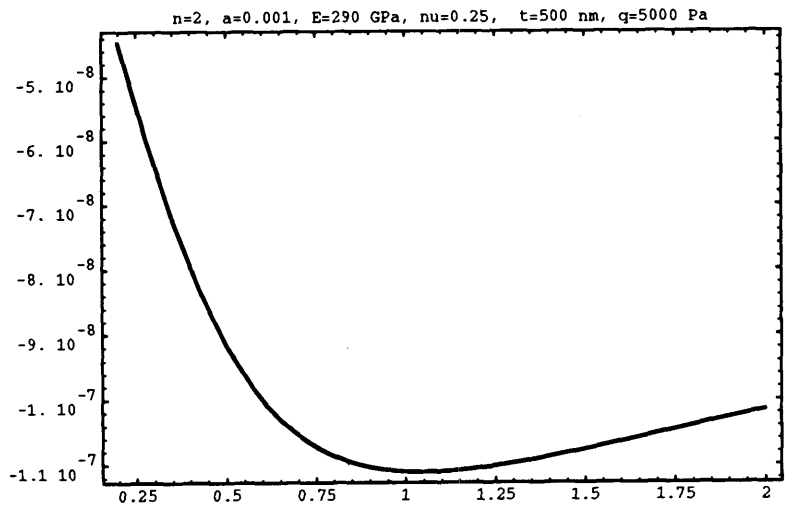

Figure 1.3: Potential energy as a function of k, $n = 2$

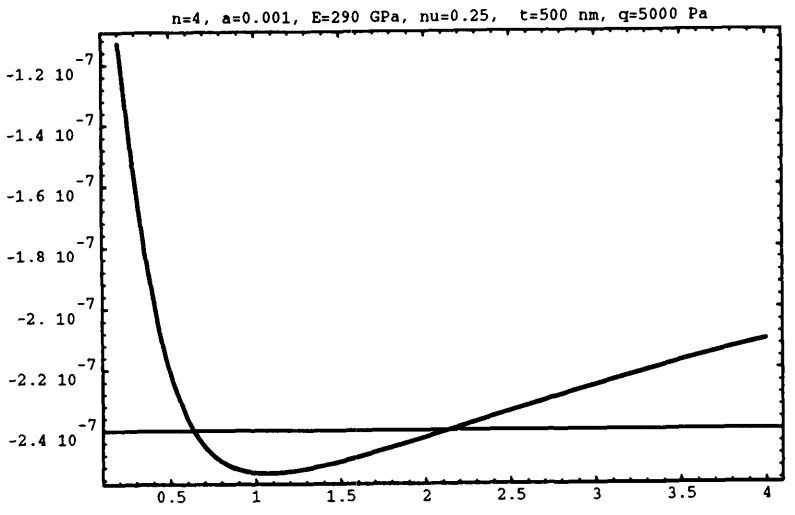

Figure 1.4: Potential energy as a function of k, $n = 4$

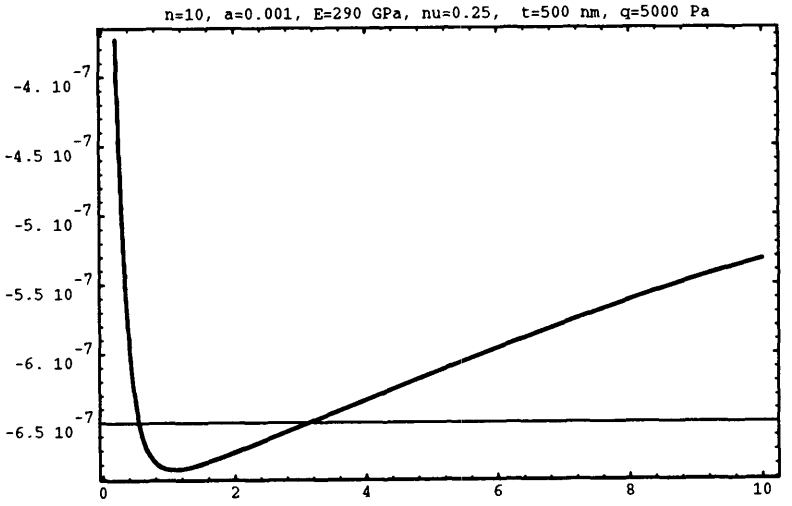

Figure 1.5: Potential energy as a function of k, $n = 10$

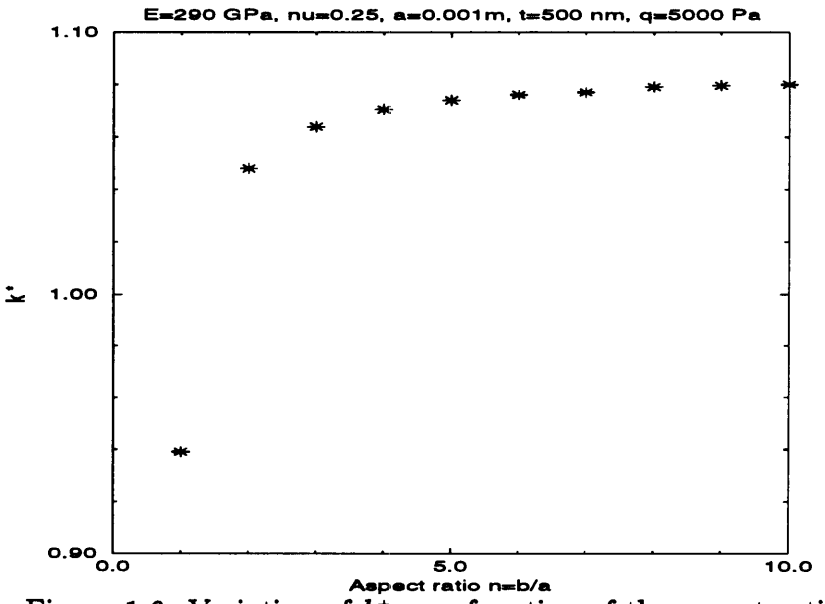

Figure 1.6: Variation of $k^\star$ as a function of the aspect ratio

cylindrical coordinates as

$$\begin{aligned}
\epsilon_r &= \frac{d\,u}{dr} + \frac{1}{2}(\frac{d\,w}{dr})^2 \\
&= c_1(a-2r) + c_2(2ar-3r^2) + 8\frac{r^2 w_0^2}{a^8}(r^2-a^2)^2, \\
\epsilon_t &= \frac{u}{r} = (a-r)(c_1+c_2 r).
\end{aligned}$$

The strain energy due solely to the stretching of the middle surface is given by

$$V = \frac{\pi E\,h}{1-\nu^2}\int_0^a (\epsilon_r^2 + \epsilon_t^2 + 2\nu\epsilon_r\epsilon_t) r\,dr, \tag{1.16}$$

$$
\begin{aligned}
V_e &= \frac{E\,h\,\pi}{(1-\nu^2)}\left(\frac{1}{4}a^4c_1^2+\frac{3}{10}a^5c_1c_2+\frac{7}{60}a^6c_2^2+\left(\frac{4}{315}+\frac{44}{315}\nu\right)a^2c_2w_0^2\right.\\
&+ \left.\left(-\frac{46}{315}+\frac{82}{315}\nu\right)ac_1w_0^2+\frac{96}{315}\frac{w_0^4}{a^2}\right).
\end{aligned}
$$

To obtain the potential energy Π, first compute the work done by the applied forces

$$
\begin{aligned}
\mathcal{W} &= 2\,\pi\int_0^a qw(r)\,r\,dr\\
&= 2\,\pi\int_0^a qw_0\left(1-\frac{r^2}{a^2}\right)^2 r\,dr\\
&= \frac{\pi w_0 q a^2}{3}.
\end{aligned}
$$

Deriving the total potential energy

$$
\begin{aligned}
\Pi &= \mathcal{V}-\mathcal{W}\\
&= \frac{E\,t\,\pi}{(1-\nu^2)}\left(\frac{1}{4}a^4c_1^2+\frac{3}{10}a^5c_1c_2+\frac{7}{60}a^6c_2^2+\left(\frac{4}{315}+\frac{44}{315}\nu\right)a^2c_2w_0^2\right.\\
&+ \left.\left(-\frac{46}{315}+\frac{82}{315}\nu\right)ac_1w_0^2+\frac{96}{315}\frac{w_0^4}{a^2}\right)-\frac{\pi w_0 q a^2}{3}
\end{aligned}
$$

and minimizing Π with respect to c_1, c_2, w_0 yields the following load-deflection relationship

$$
w_0 = \alpha_{circ}a\sqrt[3]{\frac{a\,q}{E\,t}}
$$

where

$$\alpha_{circ} = \sqrt[3]{\frac{6615}{15010 + 8500\,\nu + 5582\,\nu^2}(1 - \nu^2)}.$$

For further reference, note that

$$\begin{aligned} c_1 &= \frac{179 - 89\nu}{126}\frac{w_0^2}{a^3} \\ c_2 &= \frac{-79 + 13\nu}{42}\frac{w_0^2}{a^4}. \end{aligned} \tag{1.17}$$

Chapter 2

Comparison with numerical analysis

2.1 General methods

A commercial software, COSMOS/M, was used to numerically simulate experiments. Given

- the geometrical parameters,
  - thickness h, geometry (square, rectangle of aspect ratio n, etc...)
- the material properties,
  - Young's modulus E, Poisson's ratio ν
- the load level in the membrane q,
- the residual stress σ_0,

- the boundary conditions,

the program was able to render data of

- the load and the corresponding deflection

$$\{q_i, (w_0)_i\} \tag{2.1}$$

- and the shape of the deformed geometry

$$w = w(\vec{x}).$$

On the other hand, the models developed in chapter one yielded relations of the type

$$q = f_1\, w_0 + f_3\, w_0^3 \tag{2.2}$$

where

$$\begin{aligned} f_1 &= f_1(\sigma_0, \text{geometrical parameters}) \\ f_3 &= f_3(E, \text{geometrical parameters}). \end{aligned}$$

Therefore, if the models derived in chapter one are acceptably accurate, one should retrieve the values of E and σ_0 independently by curve-fitting the numerical data 2.1 to a third order odd polynomial and compare it to Equation 2.2.

In other words, curve-fit the data 2.1 by

$$q = \delta_1 w_0 + \delta_3 w_0^3$$

and set

$$\begin{aligned} f_1(\sigma_0, \text{geometrical parameters}) &= \delta_1 \\ f_3(E, \text{geometrical parameters}) &= \delta_3 \end{aligned}$$

which can be solved for E and σ_0 independently.

A more direct way of evaluating the models obtained in chapter one is to compare the shape of the deformed geometry given by the program to the one assumed in the energy minimization process. Both approaches will be investigated in the forthcoming sections.

The models will be compared to the numerical simulations in two steps. In Section 2.2, the residual stress will be ignored and set equal to zero in the equations. In Section 2.3, σ_0 will be set to a value of 2 MPa.

2.2 Ignoring the residual stress

If one ignores the residual stress, the load-deflection relations derived in chapter one for the different geometries can all be rewritten in the form

$$w_0 = \alpha a \sqrt[3]{\frac{a\,q}{E\,h}} \quad \text{or} \quad \frac{E\,h}{a^4 \alpha^3} w_0^3 = q \tag{2.3}$$

where

$$\alpha_s^3 = \frac{32}{\pi^6}\frac{1}{\frac{5}{64} - \frac{s^2}{r}}(1-\nu^2) \qquad \text{for a square plate}$$

$$\alpha_{inf}^3 = \frac{256}{\pi^5}(1-\nu^2) \qquad \text{for an infinite plate}$$

$$\alpha_1^3 = \frac{4}{\pi^5}(1-\nu^2)\frac{\frac{8}{\pi} + 4(n-1)}{\frac{6n-1}{64} - \frac{(s-\frac{\pi}{4}(n-1))^2}{r+2\pi^2(n-1)}} \qquad \text{for a rectangular plate, } k = 1$$

$$\alpha_k^3 = \frac{4}{\pi^5}(1-\nu^2)k^2\frac{\frac{2k}{\pi} + (n-k)}{\frac{4l}{k} - \frac{s'^2}{r'}} \qquad \text{for a rectangular plate, } k = k^\star$$

$$\alpha_{circ}^3 = \frac{6615}{15010 + 8500\,\nu + 5582\,\nu^2}(1-\nu^2) \qquad \text{for a circular plate}$$

These five different models will be compared to numerical results in the following sections.

2.2.1 Square plate

First, the validity of the displacement field will be checked by comparing the assumed deformed shape to that given by numerical analysis. Then, the numerical data will be curve-fitted to obtain the corresponding value of E.

Validity of the assumed displacement field

The following function was chosen for the deflection

$$w = w_0 \cos(\frac{\pi x}{2a}) \cos(\frac{\pi y}{2a})$$

where

$$w_0 = \alpha_s a \sqrt[3]{\frac{a\,q}{E\,h}}$$

and

$$\begin{cases} \alpha_s = \frac{16}{\pi^2}\sqrt[3]{\frac{1}{2}(1-\nu^2)}\sqrt[3]{\frac{r}{5r-64s^2}} \\ r = \frac{16}{9}(1+\nu) + \frac{\pi^2}{4}(9-\nu), \\ s = \frac{-5+3\nu}{6}. \end{cases}$$

This displacement field is compared with the numerical data in Figure 2.1. The values of the central deflection compare within 10%. The shape that was assumed in the energy minimization process was thus not suitable for this geometry since it overestimates the value of the central deflection. It is interesting to note that at locations close to the edges, the model fits the numerical data well; towards the center of the membrane, however, the deflected shape is flatter than expected on the basis of approximate theorems. It can then be expected that the model will be inaccurate in estimating the Young's modulus.

Validity of the model

To evaluate the ability of the model in yielding Young's modulus, different tests were performed for different values of Young's modulus and Poisson's ratio. The results are shown below.

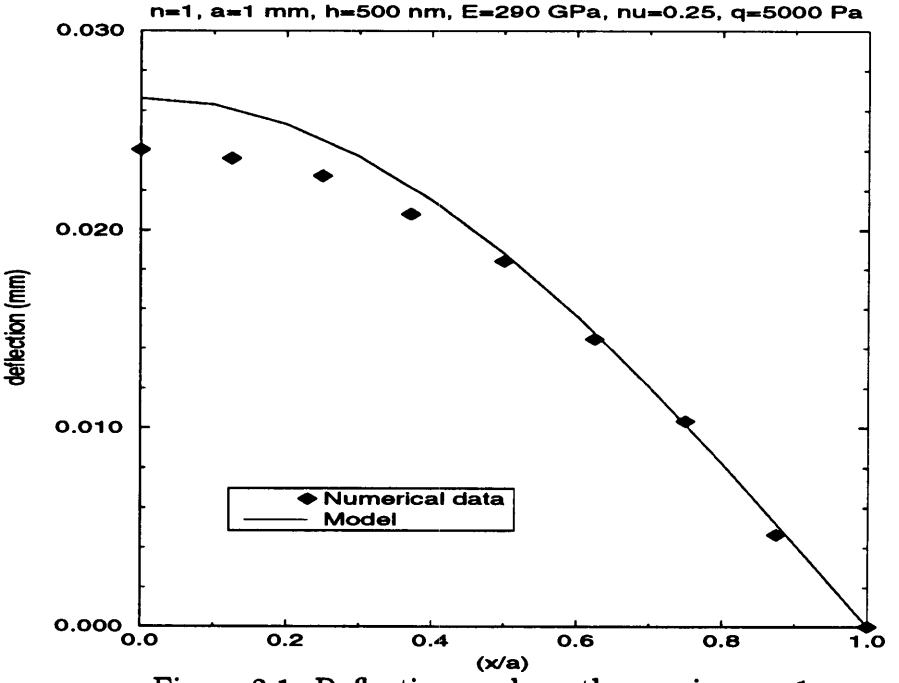

Figure 2.1: Deflection w along the x-axis; $n = 1$

- Assuming that Poisson's ratio is known and equal to 0.25, let Young's modulus vary.

ν	Input Value $E^i\,(GPa)$	Calculated $E\,(GPa)$	Error
0.25	50	67	25%
0.25	290	389	25%
0.25	450	601	25%

- For a fixed value of Young's modulus, let Poisson's ratio vary in its full range while the model assumes an average Poisson's ratio of 0.25.

ν	Input Value $E^i\,(GPa)$	Calculated $E\,(GPa)$	Error
0.0	290	327	11%
0.15	290	345	16%
0.25	290	389	25%
0.35	290	426	32%
0.45	290	498	41%

Conclusion

The error in Young's modulus is on the order of 25%, provided that Poisson's ratio is known. If Poisson's ratio takes values in its full range while the model assumes an average value of 0.25, the error increases to 41%.

The model developed in Section 1.3, therefore, fails to provide a good estimate for Young's modulus.

2.2.2 Infinite strip

The same procedure is now applied to an infinite strip. Even though this model does not account for variations along the y-axis, this section shows how it satisfactorily characterizes the behavior of rectangular membranes with "high" aspect ratio n. The results derived in Section 1.4 are compared herein to the data obtained for rectangular plates having aspect ratios two and four.

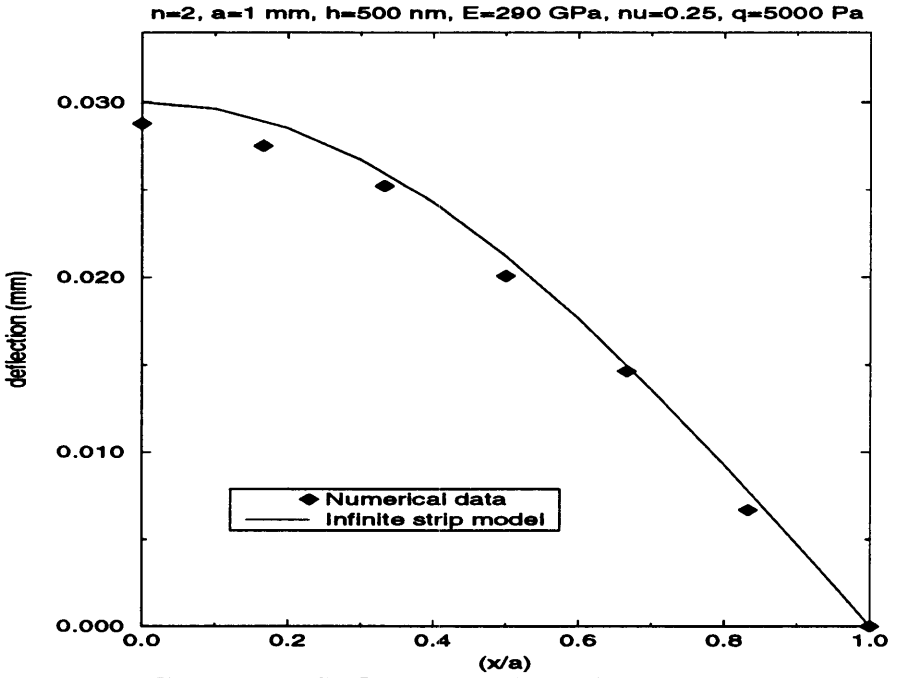

Figure 2.2: Deflection w along the x-axis, $n = 2$

Validity of the assumed displacement field

The displacement field assumed for this case was

$$w = w_0 \cos(\frac{\pi x}{2a}).$$

where

$$\begin{cases} w_0 = \alpha_{strip} a \sqrt[3]{\frac{a\,q}{E\,h}} \\ \alpha_{strip} = \sqrt[3]{\frac{256}{\pi^5}(1-\nu^2)}. \end{cases}$$

Figures 2.2 and 2.3 compare the assumed displacement field to the numerical data along the x-axis and y-axis, for a rectangular membrane of aspect ratio of two while Figures 2.4 and 2.5 refer to membranes with an aspect ratio of four.

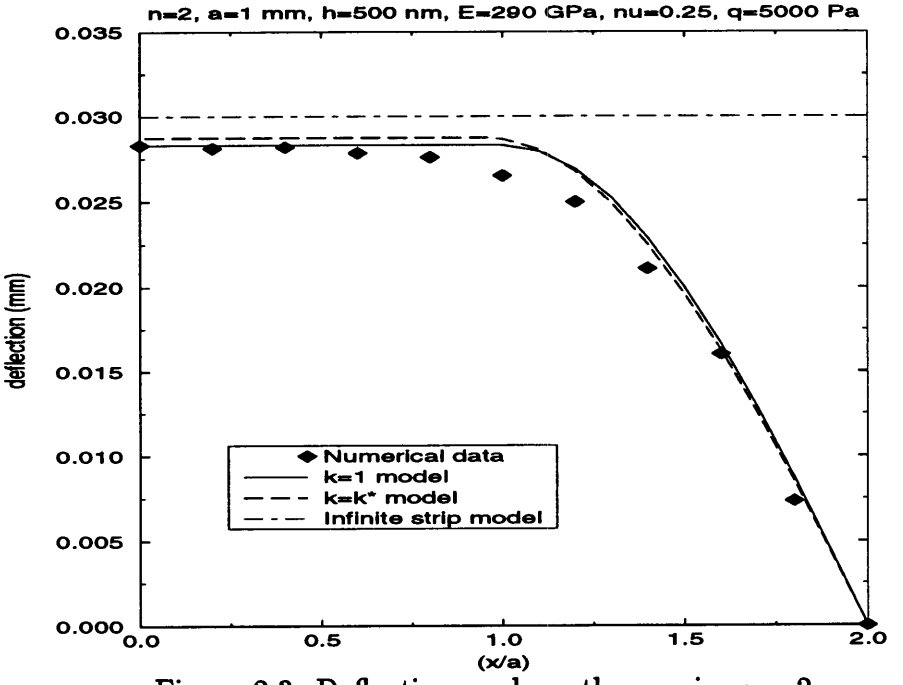

Figure 2.3: Deflection w along the y-axis, $n = 2$

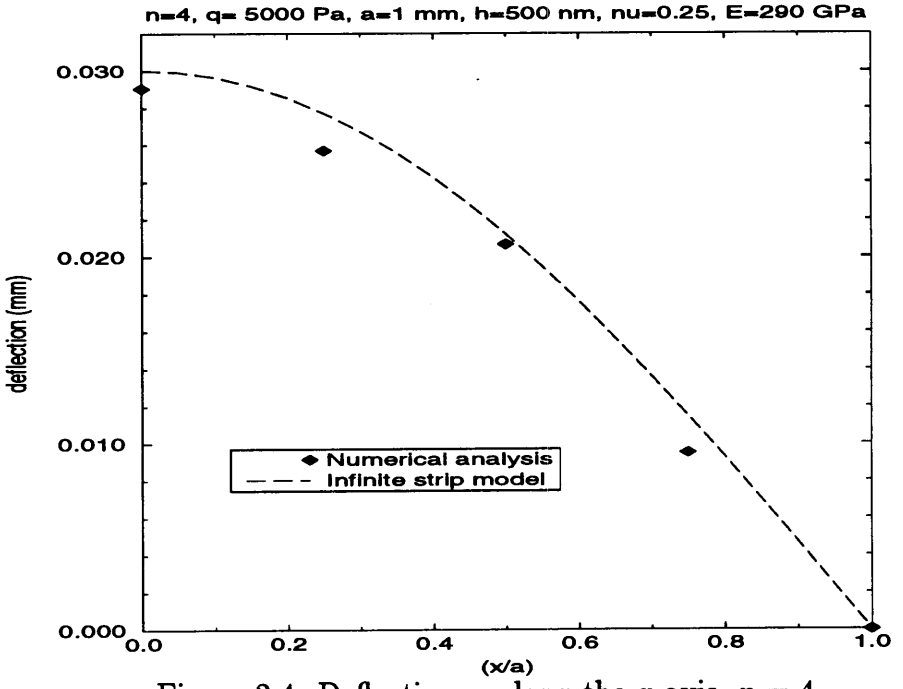

Figure 2.4: Deflection w along the x-axis, $n = 4$

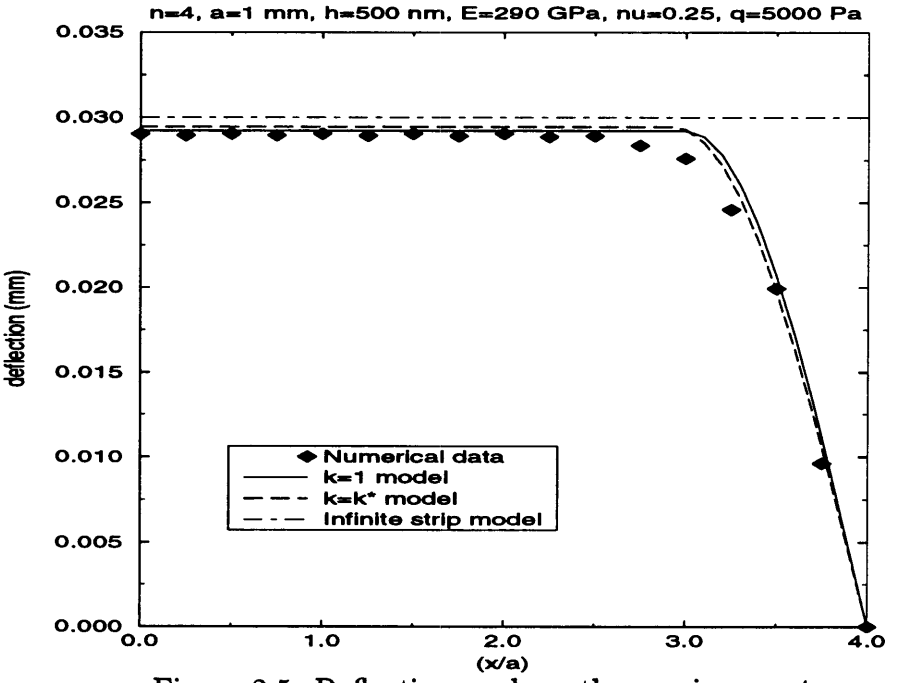

Figure 2.5: Deflection w along the y-axis, $n = 4$

The estimated value for the central deflection, w_0, is within 4% of the numerical results for an aspect ratio of two and within 3% for an aspect ratio of four. As expected, the error decreases as the aspect ratio increases.

Validity of the model

The ability of the model to yield Young's modulus was tested on membranes of aspect ratio four for different input values of Young's modulus and Poisson's ratio.

- Fix Poisson's ratio and let Young's modulus vary:

Poisson's ratio	Input Value $E^i\,(GPa)$	Calculated $E\,(GPa)$	Error
0.25	50	57	12%
0.25	160	175	9%
0.25	290	319	9%
0.25	450	520	13%

- Fix Young's modulus and let Poisson's ratio vary:

Poisson's ratio	Input Value $E^i\,(GPa)$	Calculated $E\,(GPa)$	Error
0.0	290	311	7%
0.15	290	312	8%
0.25	290	319	9%
0.35	290	335	13%
0.45	290	362	20%

Conclusion

Although the displacement field does not take the detailed bending behavior deformation along the "short" edges into account, the model developed in Section 1.4 yielded a good estimate of Young's modulus within 9% of the value specified for the numerical analysis, provided that the assumed Poisson's ratio was close to that of the material under test. If it is not, the error in E can be as high as 20% for materials with high Poisson's ratios.

2.2.3 Rectangular membrane of finite aspect ratio - $\delta = a$

Validity of the assumed displacement field

In this case, it was assumed that the displacement field could be broken into two parts as follows

$$w(x,y) = \begin{cases} w_0 \cos(\frac{\pi x}{2a}) & y \in [0,(b-a)] \\ w_0 \cos(\frac{\pi x}{2a}) \cos\frac{\pi}{2a}(y-(b-a)) & y \in [(b-a),b] \end{cases}$$

where

$$\begin{cases} w_0 = \alpha_1 a \sqrt[3]{\frac{aq}{Eh}} \\ \alpha_1 = \left(\frac{4}{\pi^5}(1-\nu^2) \frac{\left(\frac{8}{\pi}+4(n-1)\right)}{\left(\frac{6n-1}{64} - \frac{(s-\frac{\pi}{4}(n-1))^2}{r+2\pi^2(n-1)}\right)} \right)^{1/3} \end{cases}.$$

This displacement field was compared to the numerical data in Figure 2.3 and 2.5 for membranes of aspect ratio equal to two and four. The value of the central deflection compare within 0.5% of the numerical results for an aspect ratio of two and within 1.5% for an aspect ratio of four.

Validity of the model

The model was tested for two aspect ratios, various values of Young's modulus and Poisson's ratio.

- For n=2:
  - Fix Poisson's ratio and let Young's modulus vary:

ν	Input Value $E^i\,(GPa)$	Calculated $E\,(GPa)$	Error
0.25	50	50.3	0.6%
0.25	160	161.6	1.0%
0.25	290	293.0	1.0%
0.25	450	456.0	1.3%

  - Fix Young's modulus and let Poisson's ratio vary:

ν	Input Value $E^i\,(GPa)$	Calculated $E\,(GPa)$	Error
0.0	290	272	6.6%
0.15	290	281	3.1%
0.25	290	293	1.0%
0.35	290	313	7.3%
0.45	290	342	15.2%

- For n=4:
  - Fix Poisson's ratio and let Young's modulus vary:

ν	Input Value $E^i\,(GPa)$	Calculated $E\,(GPa)$	Error
0.25	50	52.9	5.5%
0.25	160	162.3	1.4%
0.25	290	294.6	1.6%
0.25	450	480.0	6.2%

– Fix Young's modulus and let Poisson's ratio vary:

ν	Input Value $E^i\,(GPa)$	Calculated $E\,(GPa)$	Error
0.0	290	287.2	1.0%
0.15	290	287.6	0.8%
0.25	290	294.6	1.6%
0.35	290	309.3	6.2%
0.45	290	334.4	13.7%

Conclusion

This model provides an accurate value of the Young's modulus (within 1% for membranes of aspect ratio equal to 2; within 6% for membranes of aspect ratio equal to four), provided that the assumed Poisson's ratio is close to that of the material under test. If this is not the case, the maximum error in E is of the order of 15% and as before, this corresponds to materials with high Poisson's ratio.

2.2.4 Rectangular membrane of finite aspect ratio - $\delta = k\,a$

Validity of the assumed displacement field

The deflection was taken of the form

$$w(x,y) = \begin{cases} w_0 \cos(\frac{\pi x}{2a}) & y \in [0,(b-k\,a)] \\ w_0 \cos(\frac{\pi x}{2a}) \cos\frac{\pi}{2a}(y-(b-k\,a)) & y \in [(b-k\,a),b] \end{cases}$$

where

$$\begin{cases} w_0 = \alpha_k a \sqrt[3]{\frac{aq}{Et}} \\ \alpha_k = \left(\frac{4(1-\nu^2)k^2}{\pi^5} \frac{\left(\frac{2k}{\pi}+(n-k)\right)}{\frac{4l}{k}-\frac{s'^2}{r'}} \right)^{\frac{1}{3}} \end{cases}$$

k depends on the aspect ratio as shown in Figure 1.6.

A comparison of the subsequent displacement field to numerical data for a membrane of aspect ratio four is shown in Figure 2.5. The value given by the model for the central deflection is within 1.3% of the numerical value.

Validity of the model

As before, one tests the ability of the model to render E by running numerical simulations with various values of E and ν.

- For an aspect ratio $n = 2$ ($k^\star = 1.05$):
  - Fix Poisson's ratio and let Young's modulus vary:

ν	Input Value $E^i\,(GPa)$	Calculated $E\,(GPa)$	Error
0.25	50	55.7	10%
0.25	160	178.7	10%
0.25	290	324.5	10%
0.25	450	504.1	11%

- Fix Young's modulus and let Poisson's ratio vary:

ν	Input Value $E^i\,(GPa)$	Calculated $E\,(GPa)$	Error
0.0	290	281.6	3%
0.15	290	285.1	2%
0.25	290	297.0	2%
0.35	290	315.7	8%
0.45	290	345.0	16%

- For an aspect ratio $n = 4$ ($k^\star = 1.07$):

  - Fix Poisson's ratio and let Young's modulus vary:

ν	Input Value $E^i\,(GPa)$	Calculated $E\,(GPa)$	Error
0.25	50	54.2	8%
0.25	160	166.1	4%
0.25	290	301.5	3%
0.25	450	491.4	8%

  - Fix Young's modulus and let Poisson's ratio vary:

ν	Input Value $E^i\,(GPa)$	Calculated $E\,(GPa)$	Error
0.0	290	294.0	1%
0.15	290	294.4	1%
0.25	290	301.5	4%
0.35	290	316.7	8%
0.45	290	342.3	15%

2.2.5 Circular plate

In the following section the same analysis is performed on a circular plate.

Validity of the assumed displacement field

The following deflection was assumed for a circular plate of radius a by Timoshenko [1].

$$w = w_0(1 - \frac{r^2}{a^2})^2$$

where w_0 was found to be

$$w_0 = \sqrt[3]{\frac{7505 + 4250\nu - 2791\nu^2}{19845}} a \sqrt[3]{\frac{a\,q}{E\,t}}.$$

This displacement field is compared with numerical data in Figure 2.6. The values of the central deflection compare within 7%. The displacement field that was assumed in this case is therefore judged inadequate. It is interesting to note that the behavior of the membrane at the edge differs greatly from that assumed. In fact, because the membrane is thin, the "zero-slope" boundary condition does not apply. Future guesses should take this aspect into account.

Validity of the model

The model is compared with numerical analysis and its ability in yielding Young's modulus is evaluated in this section.

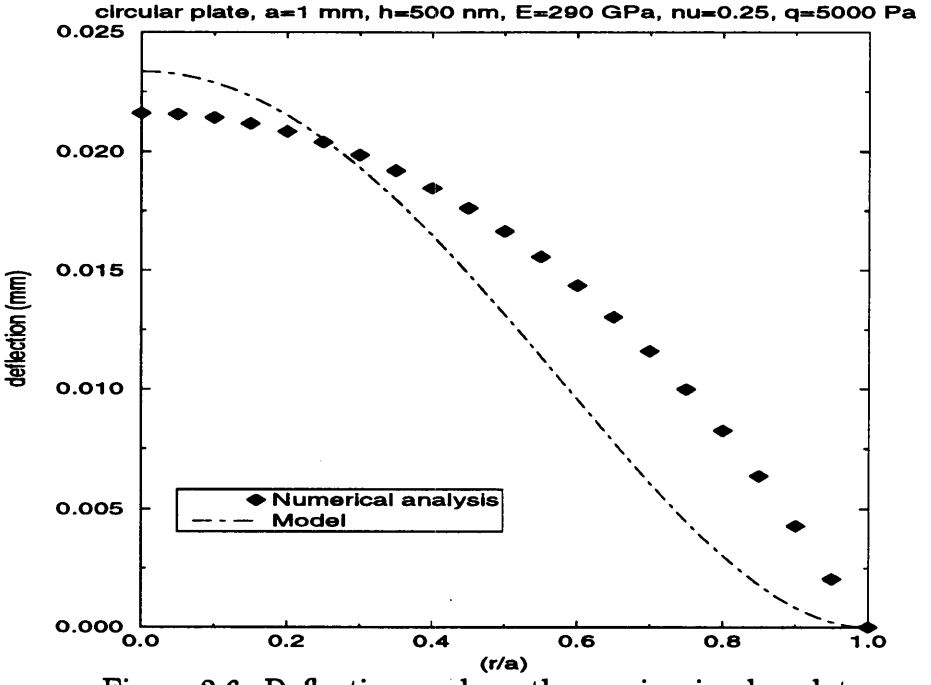

Figure 2.6: Deflection w along the r-axis, circular plate

- Fix Poisson's ratio and let Young's modulus vary:

ν	Input Value $E^i\,(GPa)$	Calculated $E\,(GPa)$	Error
0.25	50	62.6	20%
0.25	160	200.9	20%
0.25	290	364.6	20%
0.25	450	566.4	29%

- Fix Young's modulus and let Poisson's ratio vary:

ν	Input Value $E^i\,(GPa)$	Calculated $E\,(GPa)$	Error
0.05	290	302.5	4%
0.15	290	330.1	12%
0.25	290	364.6	20%
0.35	290	409.8	29%
0.45	290	471.0	38%

Conclusion

The displacement field chosen for this geometry yielded an estimate for the central deflection that differed from the numerical data by 7%. This error is reflected in the evaluation of Young's modulus which is determined within 30% of the numerical value if Poisson's ratio is known and within 40% if it varies in its full range and is assumed to be 0.25 in the model.

Because of its geometry, however, a circular membrane deflects less than a rectangular membrane of any aspect ratio, for equal characteristic length, a (radius for a circular plate, half-width for a rectangular plate). Their deflection is consequently harder to measure experimentally. Moreover, the etching processes involving epitaxial growth, rectangular membranes are more naturally obtained. Circular membranes will therefore be set aside.

2.3 Effect of the residual stress

To evaluate the influence of the residual stress, a theoretical analysis will be performed on the equation derived in chapter one. Numerical analysis will

then be used to confirm the theoretical conclusions.

2.3.1 Theoretical analysis

The following analysis will focus on rectangular membranes of any aspect ratio, n. The model for which $k^\star = 1$ is chosen to describe their load-deflection behavior.

The load-deflection relation 1.14 is rewritten in the form

$$n\frac{\pi^3}{4}\frac{tw_0}{a^2}\left\{\sigma_0 + \frac{\pi^2}{n}\frac{E}{(1-\nu^2)}\left(\frac{w_0}{a}\right)^2\left(\frac{6n-1}{64} - \frac{(s-\frac{\pi}{4}(n-1))^2}{r+2\pi^2(n-1)}\right)\right\} = q\delta,$$

where

$$\delta = \left(\frac{8}{\pi} + 4(n-1)\right).$$

In other words, one needs to compare the order of magnitude of the following expression:

$$\frac{\pi^2}{n}\left(\frac{w_0}{a}\right)^2\frac{E}{(1-\nu^2)}\left(\frac{6n-1}{64} - \frac{(s-\frac{\pi}{4}(n-1))^2}{r+2\pi^2(n-1)}\right) \tag{2.4}$$

to σ_0.

As seen in Equation 1.1, the ratio of deflection to half width is limited by the strain level in the film.

$$\left(\frac{w_0}{a}\right)^2 \sim \frac{3}{2}\varepsilon \sim 0.3\,\%.$$

For aspect ratios of one, two and four, the factor of E in Equation 2.4 is on the order of 10^{-3}. Thus, the residual stress is significant only if it is on

the order of $E/1000$. For most cases, the residual stress is much less than $E/1000$ [1]. It can therefore be ignored in the analysis.

2.3.2 Numerical analysis

Residual stresses of $1\,MPa$ and $2\,MPa$ were included in the program. The results showed no difference between this case and that without residual stress and, therefore, reinforce the above statement.

The computer program could not handle residual stresses higher than $2\,MPa$.

2.4 Strain analysis

It is assumed in the present analysis that the strains in the membrane are such that the material can be considered linearly elastic. In other words, the load was chosen such that the strains never exceed 0.2% in the membrane. This assumption is herein validated by numerical analysis. Figure 2.7 and 2.8 show the distribution of the total strain in one fourth of membranes of aspect ratio two and four respectively. The center of the membrane is located at the top left corner of the figure.

[1] The residual stress in membranes or in micro-bridges is explained by the fact that the bulk material is itself subject to residual stress. It is possible nowadays to obtain films virtually stress-free for which $\sigma_0 \sim 1MPa$.

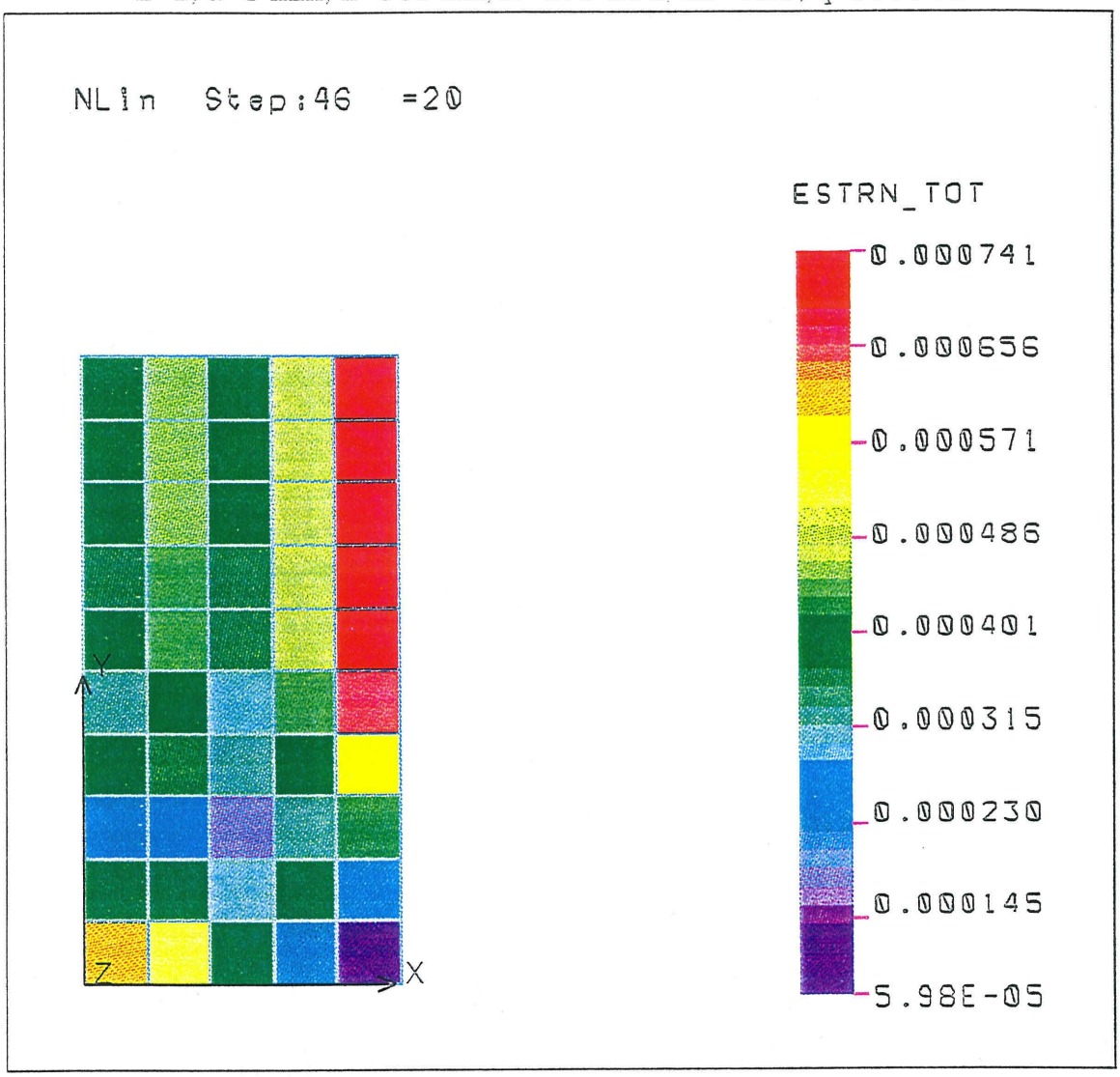

Figure 2.7: Distribution of the total strain in a membrane of aspect ratio equal to two

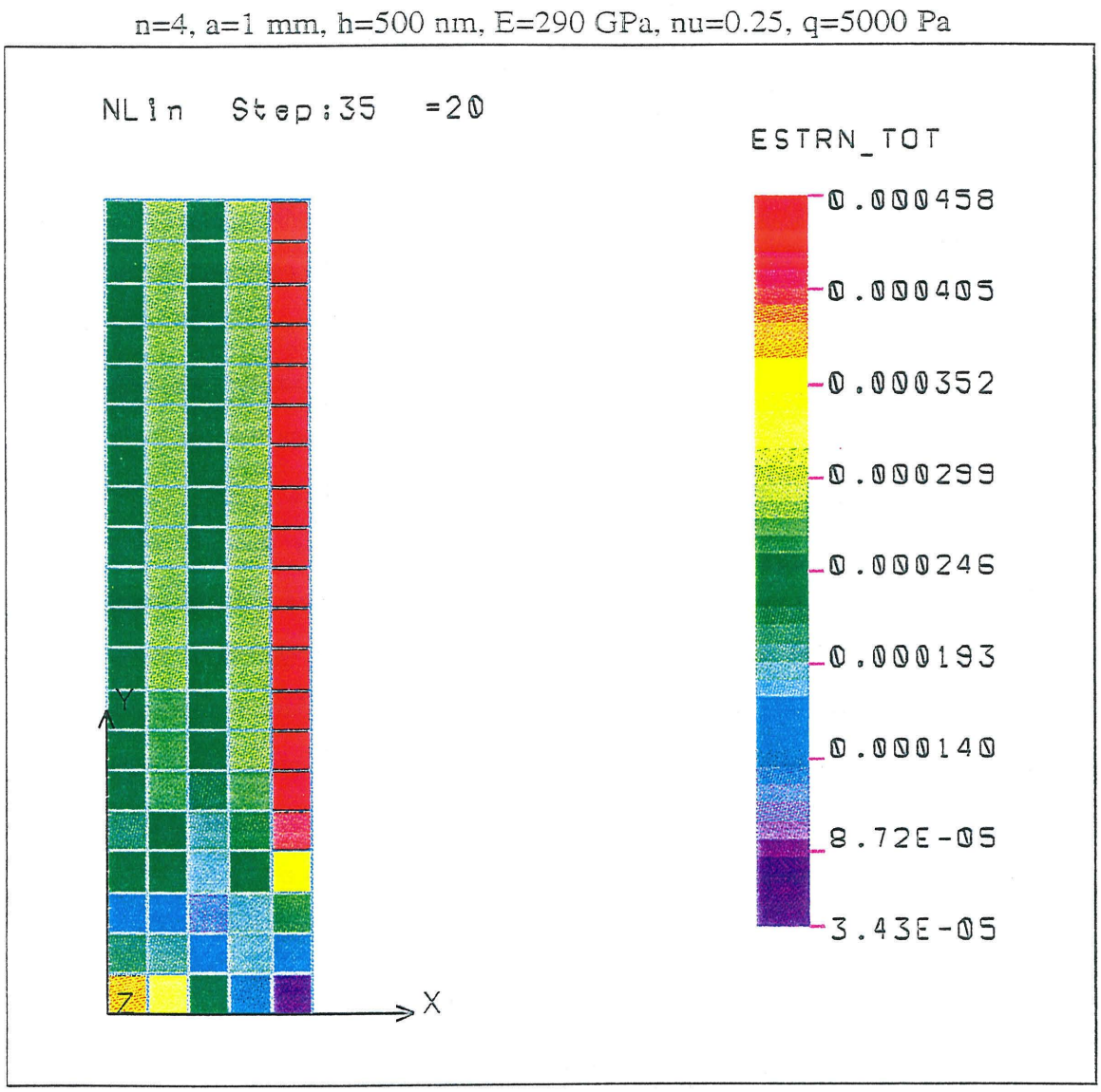

Figure 2.8: Distribution of the total strain in a membrane of aspect ratio equal to four

2.5 Discussion

2.5.1 Comparison of the proposed models

Figure 2.9 compares the value of the central deflection predicted by the different models to the numerical results for various aspect ratios, and for a known Poisson's ratio of $\nu = 0.25$. Note that when n tends to infinity in the rectangular membrane model, the solution tends to that given by an infinite strip model, as expected. In fact, for $n \geq 7$, the two values for the central deflection are within 1%.

For any aspect ratio, the rectangular plate model is superior to any other. As seen in Figure 2.9, though, the model for which $k = k^{\star}$ is better for an aspect ratio in the range {1,3}; while the model for which $k = 1$ is more accurate for aspect ratio greater than 3. This discrepancy is due to the nature of energy methods. Indeed, the minimization theorems apply to complete regions and do not provide a point-wise minimum potential energy.

It was also shown in this section that Poisson's ratio greatly influences the behavior of the membrane. Indeed, if it varies in its full range, the error in the value of E increases considerably. Chapter three will, therefore, concentrate on this effect and propose a method to determine Poisson's ratio.

2.5.2 Comparison with previously published models

The infinite strip model and the rectangular membrane model are compared with the model proposed by Tabata *et al.* [4] for which the displacement field was chosen sinusoidal along both the x and y-axes, for any aspect ratio

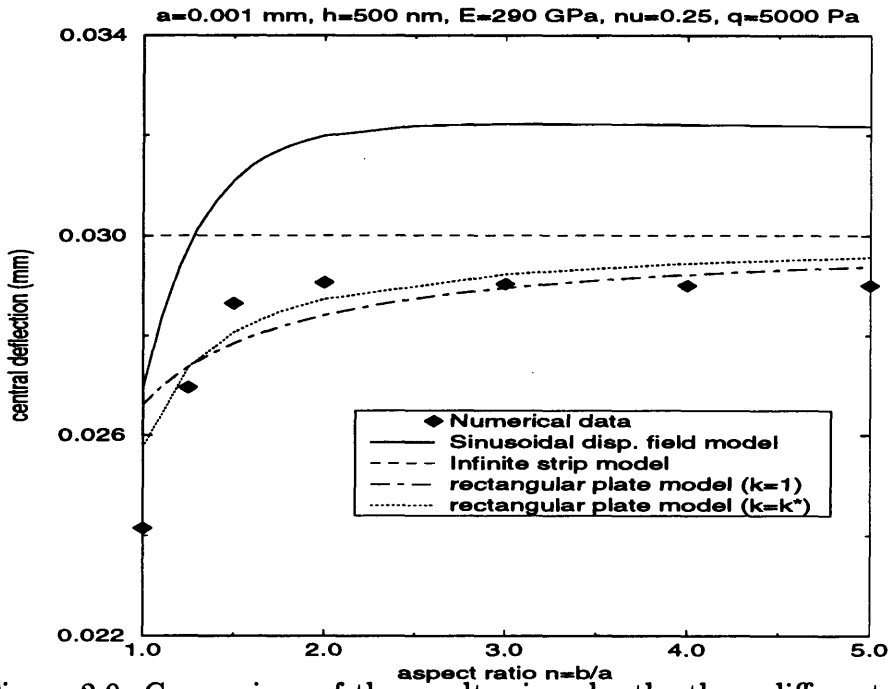

Figure 2.9: Comparison of the results given by the three different models

$n = b/a$. Namely,

$$\begin{aligned} u &= c\sin(\frac{\pi x}{a})\cos(\frac{\pi y}{2b}), \\ v &= c\sin(\frac{\pi y}{b})\cos(\frac{\pi x}{2a}), \\ w &= w_0\cos(\frac{\pi x}{2a})\cos(\frac{\pi y}{2b}). \end{aligned}$$

The central deflection predicted by this model for various aspect ratios is compared with numerical results in Figure 2.9. The displacement field assumed is not appropriate, especially to describe the deflection along the long axis (c.f. Figure 2.10). This results in an error in the predicted maximum deflection of about 10%. It is important to note that such an error in the deflection, w_0, yields a larger error in the determination of Young's modulus

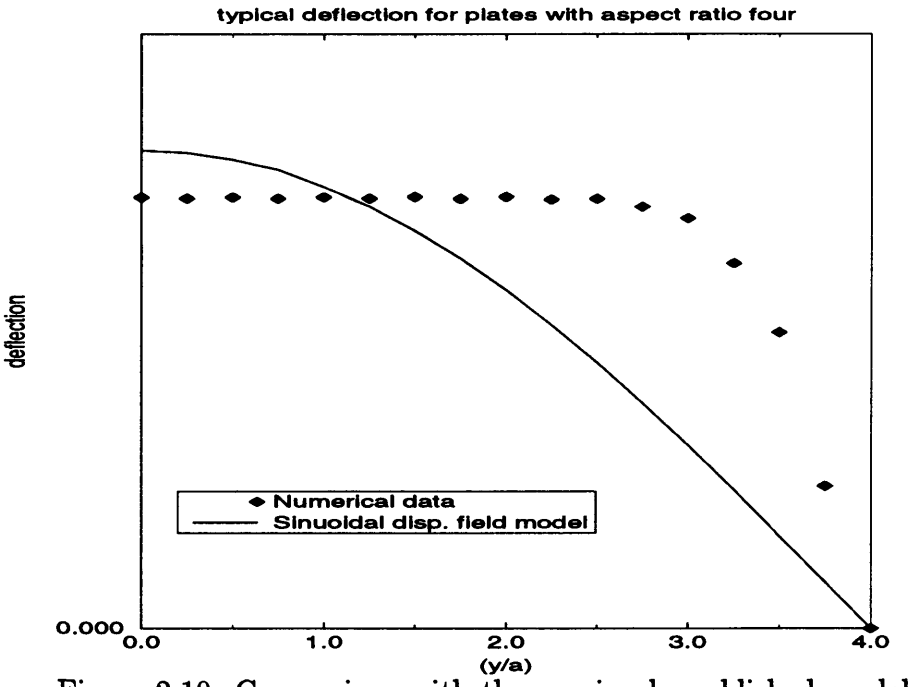

Figure 2.10: Comparison with the previously published model

E. This model is, therefore, not able to render Young's modulus with an acceptable accuracy.

The model of the rectangular plate with finite aspect ratio is believed to constitute a significant improvement over the previously published model.

Chapter 3

Influence of Poisson's ratio

3.1 Affect of Poisson's ratio

As shown by the numerical data tabulated in Section 2.2, the error in the Young's modulus is greatly increased by the fact that Poisson's ratio is unknown.

To quantify this error, rewrite Equation 1.14 neglecting the residual stress (which was shown so small as to be of no influence), using non-dimensional groups. Let

$$\frac{E}{q}\frac{t}{a}\left(\frac{w_0}{a}\right)^3 = \gamma(n,\nu),$$

where

$$\gamma(n,\nu) = (1-\nu^2)\frac{4}{\pi^5}\frac{\left(\frac{8}{\pi}+4(n-1)\right)}{\left(\frac{6n-1}{64}-\frac{(s-\frac{\pi}{4}(n-1))^2}{r+2\pi^2(n-1)}\right)},$$

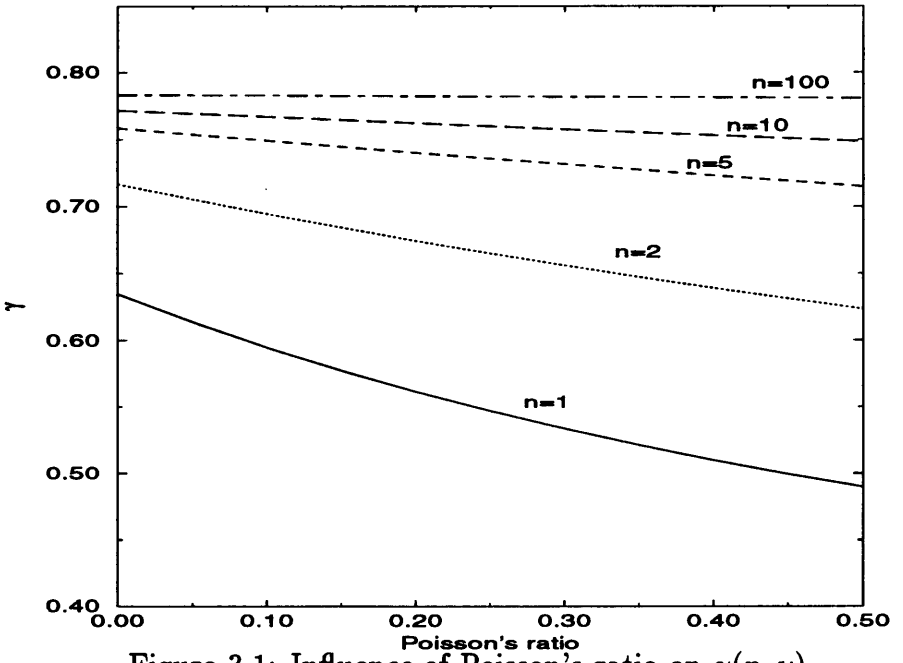

Figure 3.1: Influence of Poisson's ratio on $\gamma(n, \nu)$

where

$$\begin{cases} n = b/a, \\ r = \frac{16}{9}(1+\nu) + \frac{\pi^2}{4}(9-\nu), \\ s = \frac{-5+3\nu}{6}. \end{cases}$$

Plots of $\gamma(n, \nu)$ for different aspect ratios n are shown in Figure 3.1. This figure shows that the influence of the unknown Poisson's ratio ν on $\gamma(n, \nu)$ decreases as the aspect ratio increases. Moreover, since the error in Young's modulus is directly proportional to $\gamma(n, \nu)$, membranes of large aspect ratio should be preferred for performing the experiment.

On the other hand, it is important to note that membranes of smaller aspect ratios are easier to manufacture. Thus, one should find a compromise between membrane of high aspect ratio with an acceptable accuracy for E

for an unknown Poisson's ratio, and smaller membrane.

3.2 Method for the evaluation of ν

This section proposes a method to determine the Poisson's ratio, ν.

3.2.1 Theory

The following method has been proposed by Tabata *et al.* [5]. In order to evaluate Poisson's ratio, one can compare the load-deflection relationship of two rectangular membranes of different aspect ratio n_1 and n_2, respectively. In the general case, the load-deflection relationship reads

$$n\frac{\pi^3}{4}\sigma_0\frac{tw_0}{a^2}+\frac{E\pi^5}{4(1-\nu^2)}\frac{tw_0^3}{a^4}\left(\frac{6n-1}{64}-\frac{(s-\frac{\pi}{4}(n-1))^2}{r+2\pi^2(n-1)}\right)=q\left(\frac{8}{\pi}+4(n-1)\right).$$

It was shown that the residual stress is of no influence on the membrane behavior. Thus, the above equation may be further simplified to

$$\frac{E\pi^5}{4(1-\nu^2)}\frac{tw_0^3}{a^4}\left(\frac{6n-1}{64}-\frac{(s-\frac{\pi}{4}(n-1))^2}{r+2\pi^2(n-1)}\right)=q\left(\frac{8}{\pi}+4(n-1)\right)$$

or

$$E\,K_n\,w_0^3=q \tag{3.1}$$

with

$$K_n=\frac{t}{a^4}\frac{\pi^5}{4(1-\nu^2)}\frac{\left(\frac{6n-1}{64}-\frac{(s-\frac{\pi}{4}(n-1))^2}{r+2\pi^2(n-1)}\right)}{\left(\frac{8}{\pi}+4(n-1)\right)}$$

where K_n is a function of n and ν only.

Consider two different configurations having aspect ratios n_1 and n_2. By curve-fitting the numerical data for each to a third order polynomial, one can find the value of $E\,K_{n_1}$ and $E\,K_{n_2}$ for the membrane of aspect ratio n_1 and n_2, respectively. From these, derive

$$\frac{E\,K_{n_1}}{E\,K_{n_2}} = \frac{K_{n_1}}{K_{n_2}} = \alpha.$$

On the other hand, theoretically, one has

$$\begin{aligned} K_{n_1} &= \frac{t}{a^4}\frac{\pi^5}{4(1-\nu^2)}\frac{\left(\frac{6n_1-1}{64} - \frac{(s-\frac{\pi}{4}(n_1-1))^2}{r+2\pi^2(n_1-1)}\right)}{\left(\frac{8}{\pi}+4(n_1-1)\right)} \\ K_{n_2} &= \frac{t}{a^4}\frac{\pi^5}{4(1-\nu^2)}\frac{\left(\frac{6n_2-1}{64} - \frac{(s-\frac{\pi}{4}(n_2-1))^2}{r+2\pi^2(n_2-1)}\right)}{\left(\frac{8}{\pi}+4(n_2-1)\right)}. \end{aligned}$$

Thus,

$$\frac{K_{n_1}}{K_{n_2}} = \frac{\left(\frac{6n_1-1}{64} - \frac{(s-\frac{\pi}{4}(n_1-1))^2}{r+2\pi^2(n_1-1)}\right)}{\left(\frac{6n_2-1}{64} - \frac{(s-\frac{\pi}{4}(n_2-1))^2}{r+2\pi^2(n_2-1)}\right)}\frac{\left(\frac{8}{\pi}+4(n_2-1)\right)}{\left(\frac{8}{\pi}+4(n_1-1)\right)}.$$

Therefore, solving the equation

$$\frac{\left(\frac{6n_1-1}{64} - \frac{(s-\frac{\pi}{4}(n_1-1))^2}{r+2\pi^2(n_1-1)}\right)}{\left(\frac{6n_2-1}{64} - \frac{(s-\frac{\pi}{4}(n_2-1))^2}{r+2\pi^2(n_2-1)}\right)}\frac{\left(\frac{8}{\pi}+4(n_2-1)\right)}{\left(\frac{8}{\pi}+4(n_1-1)\right)} = \alpha \tag{3.2}$$

yields the value of the Poisson's ratio, ν. This is easily achieved graphically: For given values of n_1 and n_2, one plots K_{n_1}/K_{n_2} as a function of the Poisson's ratio. Solving Equation 3.2 then reduces to locating for which ν the K_{n_1}/K_{n_2}

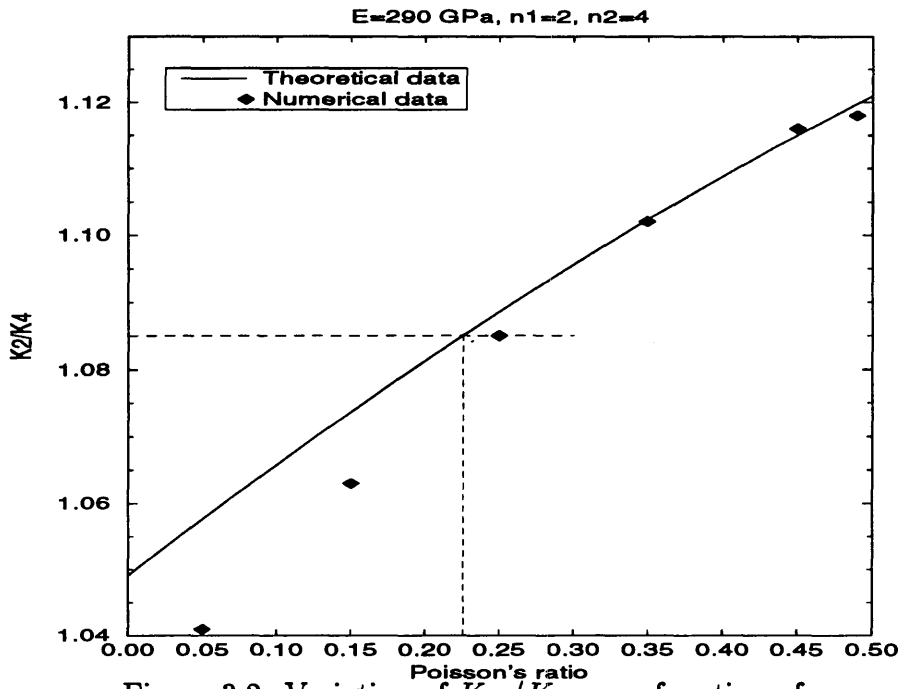

Figure 3.2: Variation of K_{n_1}/K_{n_2} as a function of ν

curve intersects with the value α. See Figure 3.2.

3.2.2 Example

From numerical data, compute the load-deflection relationship for two rectangular membranes, with material properties $E = 290\,GPa$ and $\nu = 0.25$, with aspect ratio $n_1 = 2$ and $n_2 = 4$. Note that the case $n = 1$ will be discarded since its inaccuracy was larger relative to higher aspect ratios (c.f. Section 2.2.1).

Both membranes are of thickness $t = 0.5\mu\,m$ and of half width $a = 1\,mm$.

For the membrane with aspect ratio $n = 2$, the numerical data were fitted to yield

$$2.208\,10^{17} w_0^3 = q$$

which is to be compared with Equation 3.1. Therefore, $E\,K_2 = 2.208\,10^{17}$.

For the membrane with aspect ratio $n = 4$, the numerical data render

$$2.035\,10^{17} w_0^3 = q$$

so that $E\,K_4 = 2.035\,10^{17}$. Compute the ratio

$$\frac{K_2}{K_4} = \alpha = 1.085.$$

Compare the above with the theoretical result.

$$1.085 = \frac{\left(\frac{11}{64} - \frac{(s-\frac{\pi}{4})^2}{r+2\pi^2}\right)\left(\frac{2}{\pi}+3\right)}{\left(\frac{23}{64} - \frac{(s-\frac{\pi}{4}3)^2}{r+6\pi^2}\right)\left(\frac{2}{\pi}+1\right)} \tag{3.3}$$

Using Figure 3.2, one can easily solve Equation 3.3 and find

$$\nu = 0.23\,.$$

This value is within 8% of the input value $\nu = 0.25$.

3.2.3 Additional examples

The following table lists the different values of K_2 and K_4 found numerically for different Poisson's ratios. By comparing these with the theoretical value of $\frac{K_2}{K_4}$, one can compute the corresponding Poisson's ratio ν making use of Figure 3.2.

Input ν	EK_2	EK_4	$\alpha = \frac{EK_2}{EK_4}$	ν	Error
0.00	$2.047\,10^{17}$	$1.984\,10^{17}$	1.031	N/A	N/A
0.05	$2.057\,10^{17}$	$1.976\,10^{17}$	1.041	N/A	N/A
0.15	$2.112\,10^{17}$	$1.987\,10^{17}$	1.063	0.08	50%
0.25	$2.208\,10^{17}$	$2.035\,10^{17}$	1.085	0.23	8%
0.35	$2.354\,10^{17}$	$2.137\,10^{17}$	1.102	0.34	3%
0.45	$2.577\,10^{17}$	$2.310\,10^{17}$	1.116	0.46	2%
0.49	$2.699\,10^{17}$	$2.413\,10^{17}$	1.118	0.48	2%

3.3 Discussion

It was observed in Section 2.2 that an unknown Poisson's ratio had a significant effect in the determination of the Young's modulus. A method to evaluate this Poisson's ratio was therefore proposed. However, it was found to be invalid for Poisson's ratio in the lower range $\{0, 0.25\}$. On the other hand, the method gives accurate results for higher Poisson's ratio ($\nu \in \{0.25, 0.5\}$). See Figure 3.2.

On the other hand, the Poisson's ratio is not a complete unknown: for any material, the range in which it varies is known. The value of the bulk material may be taken as a reference value for the energy method and, therefore, dramatically reduce the error in Young's modulus.

Chapter 4

Application to composite plates

Homogeneous thin films are usually difficult to manufacture or to support mechanically. On the other hand, there are simple techniques available to deposit a thin film onto a substrate, forming a composite membrane. Therefore, the methods previously developed to obtain the Young's modulus of a homogeneous film are now adapted to composite specimens. The geometry considered is also a rectangular bimaterial membrane with characteristics as follows:

- a layer of thickness h_1 possessing material properties E_1 and ν_1
- a layer of thickness h_2 with material properties E_2 and ν_2

Refer to Figure 4.1 for the definition of the geometric parameters.

Also, because the mechanical behavior of the system is greatly dependent on the thickness ratio of the two layers, three different configurations are

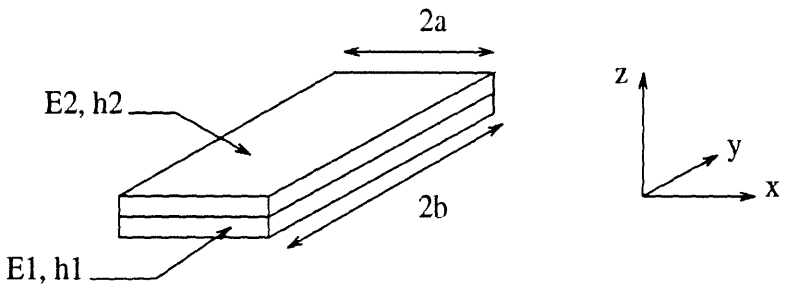

Figure 4.1: Definition of the geometric parameters for a composite membrane

examined: a) composite membranes with layers of equal thicknesses, b) the second layer is twice as thick as the substrate and finally c) the second layer is one fifth of the substrate thickness. The range of Young's modulus E_2 considered is from 50 to 500 GPa.

The problem of a bimaterial membrane may be handled in two different ways: Through the use of an effective thickness, as defined in Section 4.1, or through the use of effective material properties, as defined in Section 4.2. Section 4.3 will compare these analyses with numerical results.

4.1 Definition of the effective thickness

There are two avenues along which the effective thickness can be defined:

- Through a bending equivalent:

  Define the effective thickness h_e^b as the thickness of an object homogeneous plate with Young's modulus E_1 such that the composite plate and the homogeneous plate have the same bending stiffness D.

Therefore, h_e^b is such that

$$\begin{aligned} D &= \frac{E_1 h_e^b}{12(1-\nu^2)} \\ &= \frac{1}{(1-\nu^2)}(-\frac{1}{4}\frac{(E_1 h_1^2 + E_2 h_2^2 + 2E_2 h_1 h_2)^2}{E_1 h_1 + E_2 h_2} \\ &+ \frac{1}{3}(E_1 h_1^3 + E_2 h_2^3 + 3E_2 h_1 h_2 (h_1 + h_2)), \end{aligned}$$

which can be solved for h_e^b and written in non-dimensional form as

$$(h_e^b)^3 = h_1^3 \left(\frac{1 + 4Eh + 6Eh^2 + 4Eh^3 + E^2 h^4}{1 + Eh} \right) \tag{4.1}$$

where

$$E = \frac{E_2}{E_1},\ h = \frac{h_2}{h_1}.$$

- Through a stretch stiffness equivalent:

  Define the effective thickness h_e^s as the thickness of an object homogeneous membrane with Young's modulus E_1 such that the composite membrane and the object homogeneous membrane exhibit the same engineering strain for an equal uniaxial extensional membrane load.

  Therefore,

$$h_e^s = \frac{h_1 E_1 + h_2 E_2}{E_1} = h_1(1 + Eh) \tag{4.2}$$

  with

$$E = \frac{E_2}{E_1},\ h = \frac{h_2}{h_1}.$$

It was found in the previous sections that the behavior of a homogeneous rectangular membrane of Young's modulus E_1 and thickness h_e is satisfactory modeled by

$$w_0 = \alpha_1 a \sqrt[3]{\frac{a\,q}{E_1\,h_e}} \tag{4.3}$$

where

$$\alpha_1 = \left(\frac{4}{\pi^5}(1-\nu^2) \frac{\left(\frac{8}{\pi} + 4(n-1)\right)}{\left(\frac{6n-1}{64} - \frac{(s-\frac{\pi}{4}(n-1))^2}{r+2\pi^2(n-1)}\right)} \right)^{1/3}.$$

The only unknown in Equation 4.3 is the effective thickness h_e which can be found by curve fitting the data of load versus deflection. Once h_e is determined, Equation 4.1 or Equation 4.2 are easily solved for E_2. Recalling that E_2 is an input of the numerical code, and is therefore known, one can determine numerically which definition of the effective thickness is most appropriate.

4.2 Definition of the effective material properties

A more complete description takes into account the three dimensional aspect of the deformation.

By writing the constitutional laws for both layers and considering identical strains on both layers as leading to average stresses over the membrane thickness, on derives equivalent material properties as follows

$$\bar{\nu} = \frac{c_2}{c_1} \tag{4.4}$$

$$\bar{E} = c_1 \left\{ 1 - (\frac{c_2}{c_1})^2 \right\} \tag{4.5}$$

where

$$\begin{aligned} c_1 &= \frac{h_1}{h_1 + h_2} \left(\frac{E_1}{1 - \nu_1^2} \right) + \frac{h_2}{h_1 + h_2} \left(\frac{E_2}{1 - \nu_2^2} \right) \\ c_2 &= \nu_1 \frac{h_1}{h_1 + h_2} \left(\frac{E_1}{1 - \nu_1^2} \right) + \nu_2 \frac{h_2}{h_1 + h_2} \left(\frac{E_2}{1 - \nu_2^2} \right) \end{aligned}$$

The analysis of the mechanical behavior of the bimaterial membrane is therefore reduced to the study of an homogeneous membrane of thickness $\bar{h} = h_1 + h_2$ and material properties $\bar{E}$ and $\bar{\nu}$. The mechanical behavior of such a membrane was shown in Chapter two to be satisfactorily described by

$$w_0 = \alpha_1(\bar{\nu}) a \sqrt[3]{\frac{a\, q}{\bar{E}\,(h_1 + h_2)}} \tag{4.6}$$

4.3 Comparison with numerical analysis

Composite membranes of thickness ratios h equal to 2, 1 and 0.2 are examined in this section. For each case Young's modulus of the substrate layer will be taken equal to $290\,GPa$ while E_2 will vary in the range from $1\,GPa$ to $450\,GPa$; Poisson's ratio of the substrate material will be taken to be 0.25 while that of the complementary layer will vary in its full range.

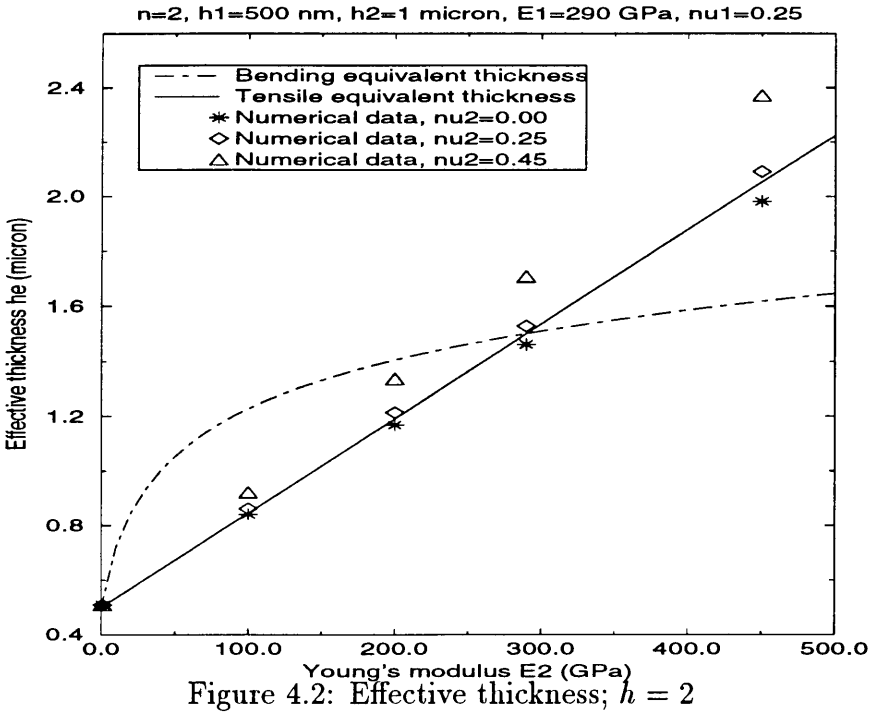

Figure 4.2: Effective thickness; $h = 2$

4.3.1 Effective thickness

The effective thickness is numerically found by curve fitting the data of load versus deflection as a third order odd polynomial and compare the latter to the theoretical equation relating the load and the deflection of a membrane of Young's modulus E_1 and thickness h_e.

By plotting the effective thickness found numerically and both effective thicknesses (defined through bending equivalent or through tensile equivalent), one can calculate easily the corresponding E_2.

Figure 4.2, 4.3 and 4.4 refer to composite membranes with thickness ratios $h = \frac{h_2}{h_1}$ equal to 2, 1 and 0.2 respectively.

Clearly, the numerical data follow a nearly linear trend which confirms the choice of a tensile equivalent thickness as an effective thickness. Indeed, the

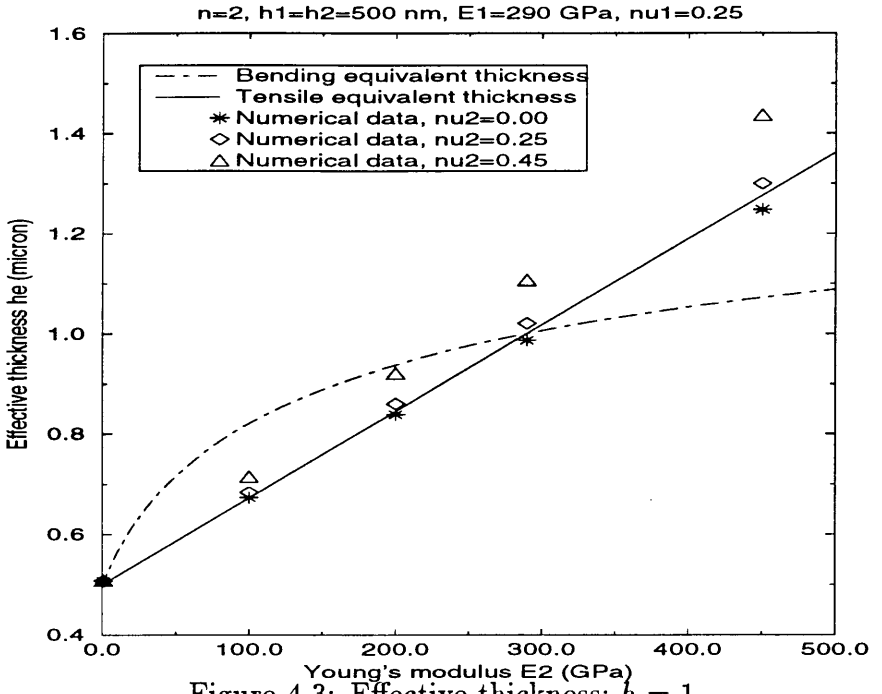

Figure 4.3: Effective thickness; $h = 1$

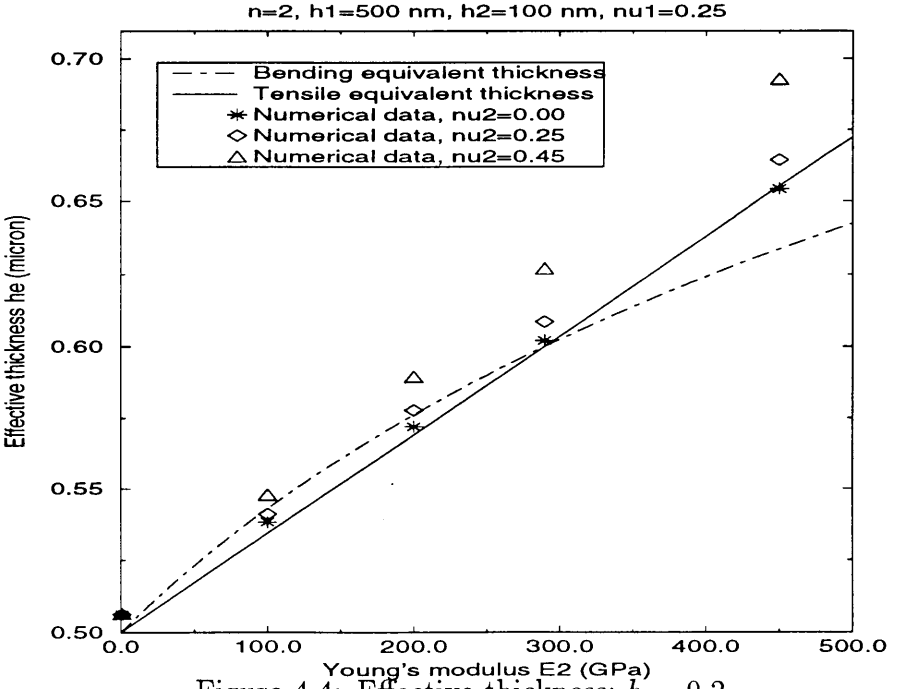

Figure 4.4: Effective thickness; $h = 0.2$

bending equivalent thickness is appropriate to describe small deformations of plates under bending. In the case considered here, the deflection is much larger than the thickness of the plate so that the deformations are controlled by in-plane stretching rather than resistance to bending; The bending-related equivalence is correspondingly poor.

If Poisson's ratio of the second layer material is in the range $\{0, 0.25\}$, Young's modulus is determined to within 3% of the value used in the numerical simulations. For higher Poisson's ratio material, the error increases to

- 21% on average for a thickness ratio of 0.2
- 18% on average for a thickness ratio of one
- 17% on average for a thickness ratio of two

The error decreases as the ratio $h = h_2/h_1$ increases. In other words, if h_2 is much larger than h_1, the error is minimized. This does not correspond, however, to the case of interest. For composite membranes, the substrate is typically much thicker than the second layer.

4.3.2 Effective material properties

For this case, the comparison with numerical analysis is performed in two steps. In a first approach, Poisson's ratios is assumed known, and the only remaining unknown in Equation 4.6 is E_2. Then, ν_2 is unknown and an average value of 0.25 is assumed by the model, while the numerical simulations let ν_2 vary in its full range. In both cases, by curve-fitting the numerical

data of load-versus-deflection and comparing this to Equation 4.6, E_2 can be determined and compared to its input value.

- First assume ν_2 known

  For thickness ratios of one and two and for low Poisson's ratio materials (ν in $\{0, 0.1\}$), Young's modulus was retrieved within 13% on average. However, as the Poisson's ratio increases, the error decreases: 3% on average for Poisson's ratio in the range $\{0.25, 0.45\}$.

  If the thickness of the layer of material under test is much thinner than the substrate the above average errors are increased to 17% for low Poisson's ratio materials and to 10% for higher Poisson's ratio materials.

- ν_2 is unknown and an average value of $\nu_2 = 0.25$ is assumed.

  If an average value of ν_2 is considered in the model, the error is on the order of 4% for low Poisson's ratio material and for any thickness ratio. For higher Poisson's ratio materials, the error increases to 20% for thickness ratios of one and two, and to 25% if the second layer is much thiner.

4.4 Discussion

For materials with Poisson's ratio in the range $\{0, 0.25\}$, the first method (Section 4.1) enables the determination of Young's modulus to within 3% of its numerical input, and to within 20% for higher Poisson's ratio materials. The second method (effective material properties; Section 4.2), however,

showed that E_2 could be retrieved within 3% of its input value for high Poisson's ratio material, providing that ν_2 is known. Thus, a combination of both analyses yields the determination of E_2 within 3% of its input value for any Poisson's ratio.

The thickness ratio is, however, a critical parameter. Indeed, if the thickness of the material under test is much thinner than the substrate, the error is increased to generate unreasonable results.

Conclusion

The deflection of a rectangular membrane undergoing large deformations under uniform pressure was successfully modeled using energy methods. Experiments were numerically simulated and data points of load versus deflection were obtained. By comparing these to the model, Young's modulus was retrieved to within 2% of the value used for the code, assuming that Poisson's ratio was known. If the latter is unknown, it was shown that assuming an average value of 0.25 yielded an error on the order of 15%. To reduce this error, a method to determine the Poisson's ratio of a homogeneous film was developed and found to be useful for ν varying from 0.25 to 0.49. In that range, the method renders Poisson's ratio to within 8% for $\nu = 0.25$ and with 2% for higher values of ν.

The model was adapted to bimaterial plates for which the substrate material is well-characterized. Young's modulus of the second layer material was found through the use of an equivalent stretch thickness, as defined in Section 4.1 or through the use of effective material properties, as defined in Section 4.2. These methods render E within 3% on average over the full range of Poisson's ratio. This error may be decreased, however, by increasing

the thickness of the second layer.

Through the comparison with numerical analysis, the models were found to be more accurate for rectangular membranes of aspect ratio equal to two or higher if Poisson's ratio is known (c.f. Section 2.2). On the other hand, it was shown in Section 3.1 that the influence of the unknown Poisson's ratio decreases with increasing aspect ratio, as expected. Narrowing of the uncertainty through bounding Poisson's ratio is also demonstrated. Rectangular membranes of aspect ratio two are therefore strongly recommended for experiments. Circular membranes should be discarded because they deflect much less than rectangular membrane for the same load level and characteristic length, as shown by numerical simulations (c.f. Section 2.2.5).

The analysis conducted in this report may be applied to the experimental study of mechanical properties of thin film. If the material under test can be obtained in the form of a homogeneous membrane of the desired thickness, it may then be tested directly using the model developed in chapter one as shown in Chapter two. The technology to manufacture these ultra-thin films is currently not available. Techniques to deposit ultra-thin films on thicker substrates, however, have been successfully developed. It was thus important to adapt this single layer film technique to a bimaterial film, which was achieved in Chapter four.

One should keep in mind that the underlying question that addresses this project is the consistency or discrepancy of material properties depending on the scale of the specimen. The material properties of a bulk material are easily found experimentally; this project provideses a method to measure those of a thin film, which is more difficult to handle. Do these properties

compare? One could now answer that question by following the forthcoming procedure. Two specimens should be tested simultaneously.

- The substrate by itself in order to characterize its mechanical behavior. This is achieved by using the method developed in Chapter one, two and three.

- The composite film: the substrate on which the material of interest is deposited. The mechanical properties of this second layer are found using the methods developed in Chapter 4.

Moreover, to ensure a consistency in the substrate thickness, these two specimens as described above should be machined simultaneously: The etching processes should leave two homogeneous films of the desired geometry on the same wafer; the material of interest should then be deposited on only one of them. The two samples can then be tested simultaneously.

If the experiment yields values of E that differs from the bulk material value, it is now possible to determine the source of the error: If the error is within 10%, one may conclude that it is due to a combination of experimental errors and modeling errors. If the difference is much greater, then one may conclude that the thickness of the film is such that homogeneity assumptions of continuum mechanics do not hold at this scale.

Bibliography

[1] Stephen Timoshenko, *"Theory of plates and shells", McGraw-Hill, 1957*

[2] Mark G. Allen, *M.S. thesis, Department of Chemical Engineering, Massachusetts Institute of Technology, May 1986*

[3] Mark G. Allen, Mehran Mehregany, Roger T. Howe and Stephan D. Senturia, *"Microfabricated structures for the in situ measurement of residual stresses, Young's modulus, and ultimate strain of thin films", Applied Physics Letter, V51(4), July 1987*

[4] Osamu Tabata, Ken Kawahata, Susumu Sugiyama, and Isemi Igarashi, *"Mechanical property measurements of thin films using load-deflection of composite rectangular membrane", Proceedings of IEEE Micro Electro Mechanical Systems, Salt Lake City, 1989*

[5] Osamu Tabata, Tomoyoshi Tsushiya and Norio Fujitsuka, *"Poisson's ratio evaluation of Thin Film for Sensor Application", Technical Digest of the 12th Sensor Symposium, Tokyo, 1994*

[6] Raymond J. Roark, *"Roark's formula for stresses and strains", 6th edition, McGraw-Hill, 1989*